Journal of Scientific Computing (2026) 108:84
https://doi.org/10.1007/s10915-026-03406-5

Semi-Lagrangian Methods for A Plasma Hybrid Model with Multi-Species Kinetic Ions and Massless Electrons

Semi-Lagrangian Methods for a Hybrid Model

Yingzhe Li[1] · **Philip J. Morrison**[2] · **Eric Sonnendrücker**[1,3]

Received: 24 October 2025 / Revised: 2 May 2026 / Accepted: 6 July 2026

Abstract
Structure preserving exact splitting based semi-Lagrangian methods are proposed for a plasma hybrid model with kinetic ions and massless electrons. Two subsystems with mass, momentum, and energy conservation are obtained by a Poisson bracket-based splitting method. For the subsystem in which the distribution functions and the fields are coupled, the second order and reversible modified implicit mid-point rule is used in time with the specially designed mean velocity. The distribution functions are not involved in the iterations and are solved by exact splittings with only one dimensional advections, which makes the proposed schemes efficient. The cancellation problem is overcome by the numerical schemes constructed. Moreover, for the case with a periodic boundary condition, the magnetic field obtained is divergence free, mass, momentum, and energy are conserved. The methods can be extended to cases with multiple ion species.

Keywords Hybrid plasma simulation · Exact splitting · Semi-Lagrangian methods

Mathematics Subject Classification 65M25 · 85-08 · 86-08 · 35Q83

✉ Yingzhe Li
yingzhe.li@ipp.mpg.de

Philip Morrison
morrison@physics.utexas.edu

Eric Sonnendrücker
eric.sonnendruecker@ipp.mpg.de

[1] Max Planck Institute for Plasma Physics, , Boltzmannstrasse 2, 85748 Garching, Germany

[2] Department of Physics and Institute for Fusion Studies, The University of Texas at Austin, Austin, TX78712, USA

[3] Technical University of Munich, Department of Mathematics, Boltzmannstrasse 3, 85748 Garching, Germany

Published online: 23 July 2026

1 Introduction

In this paper, we consider the exact splitting [3, 5] based semi-Lagrangian methods [9, 38] with the improved number of one dimensional advections for a plasma hybrid model [34, 48] with kinetic ions and massless electrons:

$$\begin{aligned} \text{kinetic ions:} \quad & \frac{\partial f}{\partial t} + \boldsymbol{v} \cdot \frac{\partial f}{\partial \boldsymbol{x}} + \frac{q}{m}(\boldsymbol{E} + \boldsymbol{v} \times \boldsymbol{B}) \cdot \frac{\partial f}{\partial \boldsymbol{v}} = 0\,, \\ \text{Faraday's law:} \quad & \frac{\partial \boldsymbol{B}}{\partial t} = -\nabla \times \boldsymbol{E}\,, \qquad \nabla \cdot \boldsymbol{B} = 0\,, \\ \text{Ohm's law:} \quad & \boldsymbol{E} = -\frac{\nabla p}{\rho} - \boldsymbol{u}_{\mathrm{e}} \times \boldsymbol{B}, \qquad \boldsymbol{u}_{\mathrm{e}} = \boldsymbol{u} - \frac{\boldsymbol{J}}{\rho}\,. \end{aligned} \tag{1}$$

Here, $f(t, \boldsymbol{x}, \boldsymbol{v})$ denotes the ion distribution function depending on time $t \in \mathbb{R}$, position $\boldsymbol{x} \in \mathbb{R}^3$ and velocity $\boldsymbol{v} \in \mathbb{R}^3$, each ion has charge q and mass m, ρ is the electron charge density with $\rho = \mathrm{e}n_e$, where n_{e} is the quasi-neutrality number density, which is equal to $n = \frac{q}{\mathrm{e}} \int f \, \mathrm{d}\boldsymbol{v}$ with the electron charge $-\mathrm{e}$, $\boldsymbol{u}_{\mathrm{e}}$ and $\boldsymbol{u} = q \int \boldsymbol{v} f \, \mathrm{d}\boldsymbol{v}/\rho$ are the electron/ion current carrying drift velocities, respectively, $\boldsymbol{E}(t, \boldsymbol{x})$ and $\boldsymbol{B}(t, \boldsymbol{x})$ stand for the electromagnetic fields, $\boldsymbol{J} = \frac{1}{\mu_0} \nabla \times \boldsymbol{B}$ denotes the plasma current with the vacuum permeability μ_0, and p is the pressure. When the electrons are isothermal, the pressure is determined by the density as $p = k_{\mathrm{B}} T_{\mathrm{e}} n_{\mathrm{e}}$, where k_{B} is the Boltzmann constant, T_{e} is the electron temperature [39]. When the electrons are adiabatic, $p = Cn^{\gamma}$ with $C = p_0/n_0^{\gamma}$ and $\gamma \neq 1$, where p_0 and n_0 are initial or equilibrium values, and γ is the ratio of specific heats [1]. As mentioned in [26], for more complex systems with gradients in the initial conditions, it is necessary to include the following separate evolution equation for the electron pressure p [39],

$$\frac{\partial p}{\partial t} + \nabla \cdot (\boldsymbol{u}_{\mathrm{e}}\, p) + (\gamma - 1)\, p\, \nabla \cdot \boldsymbol{u}_{\mathrm{e}} = 0, \quad \gamma \neq 1. \tag{2}$$

For isothermal/adiabatic electrons, the electron response is assumed to be fast and local, such that the pressure always follows the density according to an adiabatic law, the electron pressure equation is more general and can be extended when non-adiabatic effects (e.g. heat transport, kinetic corrections) are important [26, 39, 48].

Many particle-in-cell methods [14, 24, 27, 29, 32, 39] and grid based methods [34, 45, 46] have been proposed for this hybrid model. Here, we focus on the latter and use the semi-Lagrangian method [9, 38] to solve the Vlasov equation. One challenge in solving this hybrid model is to choose a suitable mean fluid velocity of the ions to advance the velocity distribution of the ions, so that the schemes have good conservation properties and are also efficient. The current advance method [32] based semi-Lagrangian methods are proposed in [45]. And in [34, 46] the exact splitting methods [8, 47] with moving (back) the frame are used to treat the nonlinearity of the mean velocity, and give efficient methods by solving the rotation part of the Vlasov equation as one dimensional advections. However, the methods in [34, 45, 46] do not preserve, momentum, energy, and other properties at the same time. The main improvement in the current work includes, 1) The specially designed mean velocity is used to overcome the cancellation problem [40], and the pressure term is considered in the exact splitting [3, 5]; 2) The mid-point rule is used for the magnetic field and pressure, such that the mass, momentum, and energy are conserved.

Semi-Lagrangian methods with exact conservation properties for kinetic equations have been proposed and developed in the literature. We list some references here. The mass and momentum conserving properties of the cubic spline-based semi-Lagrangian method [38]

for the Vlasov–Poisson equations have been given in [37]. Conservative semi-Lagrangian methods have been developed, such as in [11, 13, 50], in which the positivity of the distribution functions can be guaranteed when appropriate flux limiters are used. Efficient semi-implicit semi-Lagrangian methods that conserve mass and energy have been constructed for the Vlasov–Ampère equations in [31] using the conservative semi-Lagrangian methods [13, 50] without filters. In this work, we choose to use the cubic spline based semi-Lagrangian method [38], due to the good compromise between accuracy and efficiency [37] and the ongoing implementation for the hybrid model (1) in Gyselalib++ [6, 15].

In order to reduce the cost associated with the high-dimensional distribution functions, for semi-Lagrangian methods [9, 38], splitting techniques [33], such as directional splitting [20, 45] and Hamiltonian splitting [10, 17, 28, 35], are employed to avoid high-dimensional interpolations, thereby reducing the problem to one-dimensional advections. A useful technique is the exact splittings [3, 5], which does not have time discretization error, and reduces the rotation part of the Vlasov equation, i.e., $\frac{\partial f}{\partial t} + (\boldsymbol{v} \times \boldsymbol{B}) \cdot \frac{\partial f}{\partial \boldsymbol{v}} = 0$ into one dimensional advections. With the complicated Ohm's law in the hybrid model considered, in order to reduce the number of one dimensional advections, the splitting methods [16, 33, 41] with smaller number of sub-systems are preferable, motivated by which, in this work we present an exact splitting for $\frac{\partial f}{\partial t} + (\boldsymbol{E} + \boldsymbol{v} \times \boldsymbol{B}) \cdot \frac{\partial f}{\partial \boldsymbol{v}} = 0$ by decomposing the electric field $\boldsymbol{E}$ as the sum of the perpendicular and parallel parts to the magnetic field $\boldsymbol{B}$.

Thanks to the proposed exact splitting, the Poisson splitting [21] based on the Poisson bracket [30, 43] gives only two sub-steps when the electron pressure equation (2) is included in the model (1). For the sub-step in which the distribution functions are coupled with the magnetic field and pressure, the second order and reversible modified mid-point rule with the exact splittings [3–5] are used with a specifically chosen mean velocity, i.e., the time average of itself, such that mass, momentum, energy are conserved, and the cancellation problem [40] is overcome. And the Fourier spectral methods are used for the discretization of the fields. The proposed schemes are efficient in the sense that only one dimensional advections are needed for the update of the distribution functions thanks to the exact splitting, and the distribution functions are not involved in the iterations, which are only about fields, i.e., the schemes are semi-implicit [21, 25, 31], due to the good property of the cubic spline based semi-Lagrangian methods [38] for the velocity moments of the distribution functions. The other sub-step only involves the spatial advections, which also conserves mass, momentum, and energy exactly when mass-conserving methods, such as Fourier spectral method [36], are used.

With the time discretization and the specially chosen mean velocity mentioned above, all the above properties also hold when higher order spline based semi-Lagrangian methods [37, 38] are adopted for the distribution functions, the central finite difference method is used for the fields [39], and there are multi-species ions.

The paper is organized as follows. In Section 2, we introduce the Poisson bracket and describe the sub-steps defined by the Poisson splitting method. In Section 3, the discretizations by Fourier spectral method and semi-Lagrangian method are conducted. In Section 4, we show the schemes of the two sub-steps and the conservation properties. Section 5 presents a reduced model with one spatial dimension and two velocity dimensions, which is employed for numerical simulations. In Section 6, we validate the time accuracy order of the time semi-discretization, check the performance of the schemes, simulate the Landau damping and Bernstein waves, and present the errors of mass, momentum, and energy. In Section 7, we conclude the paper with a summary and an outlook to future works.

2 Poisson Brackets

As [27] we normalize the hybrid model (1) with the following characteristic scales,

$$
\begin{aligned}
&t = \frac{t'}{\Omega}\,,\ \boldsymbol{v} = \boldsymbol{v}'v_{\mathrm{A}}\,,\ \boldsymbol{x} = \boldsymbol{x}'\frac{v_{\mathrm{A}}}{\Omega}\,,\ \boldsymbol{B} = \boldsymbol{B}'B_{\mathrm{ref}}\,,\ \boldsymbol{E} = \boldsymbol{E}'v_{\mathrm{A}}B_{\mathrm{ref}}\,,\ p = p'm\,n_{\mathrm{ref}}\,v_{\mathrm{A}}^2,\\
&\rho = \rho' \mathrm{e}\,n_{\mathrm{ref}}\,,\ \boldsymbol{u} = \boldsymbol{u}'v_{\mathrm{A}}\,,\ \boldsymbol{J} = \boldsymbol{J}'\mathrm{e}\,n_{\mathrm{ref}}\,v_{\mathrm{A}}\,,\ \mathcal{H} = \mathcal{H}'m\,n_{\mathrm{ref}}\,v_{\mathrm{A}}^2,\\
&\kappa := \frac{k_{\mathrm{B}}T_{\mathrm{e}}}{mv_{\mathrm{A}}^2},\ \text{(isothermal electrons)},\ \mathcal{C} := \frac{p_0'}{(n_0')^{\gamma}}\ \text{(adiabatic electrons)},\\
&p_0 = p_0'm\,n_{\mathrm{ref}}\,v_A^2,\ n_0 = n_0'\,n_{\mathrm{ref}},
\end{aligned}
$$

where primed quantities are dimension-less, $\Omega = qB_{\mathrm{ref}}/m$ is the ion cyclotron frequency, B_{ref} is the characteristic magnetic field strength, $v_{\mathrm{A}} = B_{\mathrm{ref}}/\sqrt{\mu_0 m n_{\mathrm{ref}}}$ denotes the Alfvén velocity with n_{ref} the characteristic particle density, and the parameter κ denotes the ratio of $k_{\mathrm{B}}T_{\mathrm{e}}$ to mv_{A}^2 for isothermal electrons, and $\mathcal{C}$ denotes the normalized constant for adiabatic electrons with $\gamma \neq 1$. Then we obtain the following dimensionless hybrid model with general electrons in the case of single ion species with unit charge [1],

$$
\begin{aligned}
&\frac{\partial f}{\partial t} + \boldsymbol{v}\cdot\frac{\partial f}{\partial \boldsymbol{x}} + (\boldsymbol{E} + \boldsymbol{v}\times\boldsymbol{B})\cdot\frac{\partial f}{\partial \boldsymbol{v}} = 0\,,\\
&\frac{\partial \boldsymbol{B}}{\partial t} = -\nabla\times\boldsymbol{E}\,,\quad \nabla\cdot\boldsymbol{B} = 0\,,\\
&\boldsymbol{E} = -\frac{\nabla p}{\rho} - \boldsymbol{u}_{\mathrm{e}}\times\boldsymbol{B},\\
&\frac{\partial p}{\partial t} + \nabla\cdot(\boldsymbol{u}_{\mathrm{e}}\,p) + (\gamma-1)\,p\,\nabla\cdot\boldsymbol{u}_{\mathrm{e}} = 0,\quad \boldsymbol{u}_{\mathrm{e}} = \boldsymbol{u} - \frac{\boldsymbol{J}}{\rho},\quad \gamma\neq 1.
\end{aligned}
\tag{3}
$$

where $\rho = \int f\,\mathrm{d}\boldsymbol{v}$ and $\boldsymbol{u} = \int \boldsymbol{v} f\,\mathrm{d}\boldsymbol{v}/\rho$. In the case with the isothermal/adiabatic electrons, the pressure p is determined with the density ρ as $p = \kappa\rho$ for isothermal electrons, and $p = \mathcal{C}\rho^{\gamma}$ for adiabatic electrons with $\gamma \neq 1$.

In the following, we focus on the case with general electrons, the case with isothermal or adiabatic electrons can be considered similarly. There is a Poisson bracket for model (3) proposed in [27, 30] based on the results in [43]. The Poisson bracket $\{\cdot,\cdot\} : V\times V\to V$, for the model (3) is, where V denotes the vector space of functionals $\mathcal{F} : (f, \boldsymbol{B}, \boldsymbol{p}) \mapsto \mathbb{R}$ on the space of unknowns,

$$
\{\mathcal{F},\mathcal{G}\} = \{\mathcal{F},\mathcal{G}\}_{xv} + \{\mathcal{F},\mathcal{G}\}_{pvb}. \tag{4}
$$

The detailed expressions of these two sub-brackets are provided in the appendix 8.1. The energy of the dimensionless hybrid model (3) is

$$
\mathcal{E} = \frac{1}{2}\int |\boldsymbol{v}|^2 f\,\mathrm{d}\boldsymbol{x}\,\mathrm{d}\boldsymbol{v} + \frac{1}{2}\int |\boldsymbol{B}|^2\,\mathrm{d}\boldsymbol{x} + \int \frac{p}{\gamma-1}\,\mathrm{d}\boldsymbol{x} =: K_f + K_B + K_p,\quad \gamma\neq 1. \tag{5}
$$

With energy (5) and Poisson bracket (4), the hybrid model (3) can be written in a Poisson bracket form $\dot{\mathcal{Z}} = \{\mathcal{Z},\mathcal{E}\}$ with $\mathcal{Z} = (f, \boldsymbol{B}, p)$. Poisson brackets provide a theoretical foundation for constructing structure-preserving methods. For example, geometric particle-in-cell methods have been constructed based on Poisson brackets in [7, 19, 22, 23, 49] for the Vlasov–Maxwell equations.

[1] We omit the primes on normalized quantities for simplicity in the remaining parts of this work.

The time discretization is obtained by the Poisson splitting methods [21] based on the decomposition of the full bracket (4) into two parts, which gives two sub-steps conserving mass $\mathcal{M} = \int f \, \mathrm{d}\boldsymbol{x} \, \mathrm{d}\boldsymbol{v}$, momentum $\mathcal{P} = \int \boldsymbol{v} f \, \mathrm{d}\boldsymbol{x} \, \mathrm{d}\boldsymbol{v}$, and energy $\mathcal{E}$. The first sub-step called pvb, corresponding to the sub-bracket $\{\mathcal{F}, \mathcal{G}\}_{pvb}$, is

$$\begin{aligned} &\frac{\partial f}{\partial t} + (\boldsymbol{E} + \boldsymbol{v} \times \boldsymbol{B}) \cdot \frac{\partial f}{\partial \boldsymbol{v}} = 0 \,, \\ &\frac{\partial \boldsymbol{B}}{\partial t} = -\nabla \times \boldsymbol{E}, \quad \boldsymbol{E} = -\frac{\nabla p}{\rho} - \boldsymbol{u}_{\mathrm{e}} \times \boldsymbol{B}, \\ &\frac{\partial p}{\partial t} + \nabla \cdot (\boldsymbol{u}_{\mathrm{e}} \, p) + (\gamma - 1) \, p \, \nabla \cdot \boldsymbol{u}_{\mathrm{e}} = 0, \quad \boldsymbol{u}_{\mathrm{e}} = \boldsymbol{u} - \frac{\boldsymbol{J}}{\rho}, \quad \gamma \neq 1. \end{aligned} \tag{6}$$

The second sub-step called xv, corresponding to sub-bracket $\{\mathcal{F}, \mathcal{G}\}_{xv}$, is

$$\frac{\partial f}{\partial t} = -\boldsymbol{v} \cdot \nabla_x f. \tag{7}$$

We can derive the equation of $\boldsymbol{J}_f = \int \boldsymbol{v} f \, \mathrm{d}\boldsymbol{v}$ or $\boldsymbol{u}$ from the sub-step pbv (6)

$$\frac{\partial \boldsymbol{J}_f}{\partial t} = -\nabla p + (\nabla \times \boldsymbol{B}) \times \boldsymbol{B}, \text{ or } \frac{\partial \boldsymbol{u}}{\partial t} = -\frac{\nabla p}{\rho} + \frac{(\nabla \times \boldsymbol{B}) \times \boldsymbol{B}}{\rho}, \tag{8}$$

i.e., the contributions of the two terms, $\boldsymbol{v} \times \boldsymbol{B}$ and $-\boldsymbol{u} \times \boldsymbol{B}$, cancel each other in the time evolution equation of the $\boldsymbol{J}_f$ or $\boldsymbol{u}$. This property needs to be preserved after numerical discretization, otherwise the so-called cancellation problem would arise [40].

3 Discretization

In this section, we present the details of the discretization, which will be used in the discretization of sub-steps in Section 4. Periodic boundary conditions are imposed in space. Fourier spectral methods [36] and semi-Lagrangian methods [38] are presented in detail. For the time discretization of the unknown a, we denote its approximation at n-th time step, i.e., at $t = n\Delta t$, as a^n, where Δt is the time step size. For field unknowns a, $a^{n+\frac{1}{2}} = \frac{1}{2}(a^n + a^{n+1})$.

Here, we define the notations used in the phase-space discretization. We consider the domain $\Omega = \Omega_x \times \Omega_v$, in which $\Omega_x = \Pi_{\alpha=1}^3 [0, L_\alpha]$, $\Omega_v = \Pi_{\alpha=1}^3 [-v_l^\alpha, v_r^\alpha]$, L_α, v_l^α, and v_r^α are real numbers, v_l^α and v_r^α are chosen such that it is also reasonable to assume periodic boundary conditions in velocity. We use uniform grids in space and velocity. The grids and duals of grids (in Fourier spaces) [5] along the α-th space direction are

$$\mathbb{G}^{x_\alpha} = \Delta x_\alpha \, [0, M_\alpha - 1] \,, \quad \Delta x_\alpha = L_\alpha / M_\alpha, \quad \hat{\mathbb{G}}^{x_\alpha} = \frac{2\pi}{L_\alpha} \left[\!\!\left[-\left\lfloor \frac{M_\alpha - 1}{2} \right\rfloor, \left\lfloor \frac{M_\alpha}{2} \right\rfloor \right]\!\!\right], \tag{9}$$

where M_α denotes the number of grid points in α-th space direction, the variable implicitly associated with $\mathbb{G}^{x_\alpha}$ (resp. $\hat{\mathbb{G}}^{x_\alpha}$) is denoted as x_α (resp. ξ_α). The grids in the α-th direction of the velocity are

$$\mathbb{G}^{v_\alpha} = \Delta v_\alpha \, [0, N_\alpha - 1] \,, \quad \Delta v_\alpha = \frac{v_r^\alpha - v_l^\alpha}{N_\alpha},$$

where N_α denotes the number of grid points in the α-th velocity direction, and the variable implicitly associated with $\mathbb{G}^{v_\alpha}$ is denoted as v_α. We also define $\Delta \boldsymbol{x} := \Delta x_1 \Delta x_2 \Delta x_3$, and

$\Delta \boldsymbol{v} := \Delta v_1 \Delta v_2 \Delta v_3$. The variable x (resp. v) is implicitly associated with the three dimensional grids $\mathbb{G}^x = \Pi_{\alpha=1}^3 \mathbb{G}^{x_\alpha}$ (resp. $\mathbb{G}^v = \Pi_{\alpha=1}^3 \mathbb{G}^{v_\alpha}$) [22]. Similarly for the frequency, we have the variable ξ implicitly associated with the duals of grids $\hat{\mathbb{G}}^x = \Pi_{\alpha=1}^3 \hat{\mathbb{G}}^{x_\alpha}$.

For a scalar function $s(\boldsymbol{x})$, its discretization on $\mathbb{G}^x$ is denoted as $\mathbf{s}$, for which we define the discrete partial Fourier transforms $\mathcal{F}_\alpha$ along x_α direction in appendix 8.2 [4], and its value at grid $\mathsf{x} \in \mathbb{G}^x$ is $\mathbf{s}_\mathsf{x}$. For the pressure p and the α-th component of the magnetic field $B_\alpha(\boldsymbol{x})$, corresponding discretizations on grids $\mathbb{G}^x$ are denoted as $\mathbf{p}$ and $\mathbf{B}_\alpha$, respectively. And the value of the discretization $\mathbf{B}$ at grid $\mathsf{x} \in \mathbb{G}^x$ is denoted as $\mathbf{B}_\mathsf{x} = \left(\mathbf{B}_{1,\mathsf{x}}, \mathbf{B}_{2,\mathsf{x}}, \mathbf{B}_{3,\mathsf{x}}\right)^\top$.

The definition of partial discrete Fourier transformation, discrete ∇ for a scalar function $\mathbf{s}$, discrete $\nabla\times$ and $\nabla\cdot$ for a vector function $\mathbf{B}$, and the proof of $\nabla \times \nabla = 0$ and $\nabla \cdot \nabla \times = 0$ can be found in appendix 8.3 [7].

We denote the approximation of the distribution function at uniform grids $\mathbb{G}^x \times \mathbb{G}^v$ as $\mathbf{f}$. The Fourier coefficients $\hat{\mathbf{f}}$ defined on the grids $\hat{\mathbb{G}}^x \times \mathbb{G}^v$ are obtained by discrete Fourier transform in space for $\mathbf{f}$. With $\mathbf{f}$, we can take the discrete velocity moments and get $\boldsymbol{\rho}$, $\mathbf{J}_{f,\alpha}$, $\mathbf{u}$, and $\mathbf{u}_e$,

$$\boldsymbol{\rho}_\mathsf{x} = \sum_{\mathsf{v}\in\mathbb{G}^v} \mathbf{f}_{\mathsf{xv}}\, \Delta \boldsymbol{v}, \quad \mathbf{J}_{f,\alpha,\mathsf{x}} = \sum_{\mathsf{v}\in\mathbb{G}^v} \mathbf{f}_{\mathsf{xv}}\, \mathsf{v}_\alpha \Delta \boldsymbol{v},$$
$$\mathbf{u}_{\alpha,\mathsf{x}} = \mathbf{J}_{f,\alpha,\mathsf{x}}/\boldsymbol{\rho}_\mathsf{x}, \quad \mathbf{u}_{e,\alpha,\mathsf{x}} = \mathbf{u}_{\alpha,\mathsf{x}} - (\nabla \times \mathbf{B})_\mathsf{x}/\boldsymbol{\rho}_\mathsf{x},$$

which are associated with their Fourier coefficients $\hat{\boldsymbol{\rho}}$, $\hat{\mathbf{J}}_{f,\alpha}$, $\hat{\mathbf{u}}$, and $\hat{\mathbf{u}}_e$ via discrete Fourier transform.

Computation of the one-dimensional advections. In this work, the distribution function is updated via only one dimensional advections, so here we present the details of solving the one dimensional transport equation of the function $f(t, z)$

$$\frac{\partial f}{\partial t} + c\frac{\partial f}{\partial z} = 0, \quad c \in \mathbb{R}. \tag{10}$$

The domain is $[a, b]$ and a periodic boundary condition is assumed. When we consider a specific advection along some space direction, the variable z would represent corresponding components of $\boldsymbol{x}$. We use a uniform grids $\mathbb{G}^z$ with cell number M, and its duals $\hat{\mathbb{G}}^z$ as (9), the variable implicitly associated with $\mathbb{G}^z$ (resp. $\hat{\mathbb{G}}^z$) is denoted as z (resp. β), The discretization of f, i.e., $\mathbf{f}$, is a function defined on $\mathbb{G}^z$. When we use Fourier spectral method, $\mathbf{f}$ is updated in time as

$$\mathbf{f}^{n+1} = \mathcal{F}_z^{-1} e^{-\mathrm{i}c\Delta t\beta} \mathcal{F}_z\, \mathbf{f}^n, \tag{11}$$

where $\mathcal{F}_z$ is the discrete Fourier transform,

$$\mathcal{F}_z : \mathbb{C}^{\mathbb{G}^z} \to \mathbb{C}^{\hat{\mathbb{G}}^z} : \mathbf{f} \to \hat{\mathbf{f}} = \sum_{z\in\mathbb{G}^z} f_z e^{-\mathrm{i}z\beta}.$$

Lemma 1 *For the translation* (11) *conducted with the Fourier spectral method, we have* $\sum_{\mathsf{z}\in\mathbb{G}^z} \mathbf{f}_\mathsf{z}^{n+1} = \sum_{\mathsf{z}\in\mathbb{G}^z} \mathbf{f}_\mathsf{z}^n$.

Proof Based on the definition of discrete Fourier transform [36], we have

$$\sum_{\mathsf{z}\in\mathbb{G}^z} \mathbf{f}_\mathsf{z}^{n+1} = \hat{\mathbf{f}}_0^{n+1}, \quad \sum_{\mathsf{z}\in\mathbb{G}^z} \mathbf{f}_\mathsf{z}^n = \hat{\mathbf{f}}_0^n.$$

As $\beta = 0$, $\hat{\mathbf{f}}_0^n = \hat{\mathbf{f}}_0^{n+1}$ and $\sum_{\mathsf{z}\in\mathbb{G}^z} \mathbf{f}_\mathsf{z}^{n+1} = \sum_{\mathsf{z}\in\mathbb{G}^z} \mathbf{f}_\mathsf{z}^n$. □

When we use the cubic spline based semi-Lagrangian method [38], first we reconstruct a continuous function $\mathcal{I}\mathbf{f}^n(z) := \sum_{z\in\mathbb{G}^z} \mathbf{e}_z C(z-\mathsf{z})$ using $\mathbf{f}^n$, where $\mathbf{e}_z$ is the coefficient of $C(z-\mathsf{z})$, and $C(z)$ is the cubic B-spline,

$$C(z) = \frac{1}{6}\begin{cases} (2-|z|/\Delta z)^3 & \text{if} \quad \Delta z \le |z| < 2\Delta z \\ 4-6(|z|/\Delta z)^2 + 3(|z|/\Delta z)^3 & \text{if} \quad 0 \le |z| < \Delta z \\ 0 & \text{else} \end{cases}$$

and the coefficients $\mathbf{e}$ of the cubic splines are obtained by a fast solver given in [37] when periodic boundary conditions are imposed. When the support of $C(z-\mathsf{z})$ extends beyond the domain, we handle it using the periodicity assumption. Then the distribution function is updated as

$$\mathbf{f}_{\mathsf{z}}^{n+1} = \mathcal{I}\mathbf{f}^n(\mathsf{z} - c\Delta t). \tag{12}$$

The cubic splines on an uniform grid $\mathbb{G}^z$ of the velocity domain $\mathbb{R}$ have the following properties on the moments, i.e., a generalization of partition of unity, which is proved with the partition of unity, the recurrence definition of splines, and by induction [44].

Proposition 1 *[44] For the cubic spline $C(z)$, we have*

$$\int_{\mathbb{R}} z^s\, C(z)\,\mathrm{d}z = \sum_{\mathsf{z}\in\mathbb{G}^z} (\mathsf{z}+r)^s\, C(\mathsf{z}+r)\,\Delta z, \quad \forall r \in \mathbb{R}, s = 0, 1, 2.$$

Based the Proposition 1, we have the following result about change of variables.

Proposition 2

$$\sum_{\mathsf{z}\in\mathbb{G}^z} \mathsf{z}^s\, C(\mathsf{z}+r)\,\Delta z = \sum_{\mathsf{z}\in\mathbb{G}^z} (\mathsf{z}-r)^s\, C(\mathsf{z})\,\Delta z, \quad \forall r \in \mathbb{R}, s = 0, 1, 2.$$

Proof We here focus on the case with $s = 2$, the cases with $s = 0, 1$ can be proved similarly.

$$\begin{aligned}
&\sum_{\mathsf{z}\in\mathbb{G}^z} \mathsf{z}^2\, C(\mathsf{z}+r)\,\Delta z = \sum_{\mathsf{z}\in\mathbb{G}^z} (\mathsf{z}+r-r)^2\, C(\mathsf{z}+r)\Delta z \\
&= \sum_{\mathsf{z}\in\mathbb{G}^z} (\mathsf{z}+r)^2\, C(\mathsf{z}+r)\,\Delta z + \sum_{\mathsf{z}\in\mathbb{G}^z} r^2\, C(\mathsf{z}+r)\,\Delta z - \sum_{\mathsf{z}\in\mathbb{G}^z} 2r(\mathsf{z}+r)\, C(\mathsf{z}+r)\,\Delta z \\
&= \sum_{\mathsf{z}\in\mathbb{G}^z} \mathsf{z}^2\, C(\mathsf{z})\,\Delta z + \sum_{\mathsf{z}\in\mathbb{G}^z} r^2\, C(\mathsf{z})\,\Delta z - \sum_{\mathsf{z}\in\mathbb{G}^z} 2\,r\mathsf{z}C(\mathsf{z})\,\Delta z \\
&= \sum_{\mathsf{z}\in\mathbb{G}^z} (\mathsf{z}-r)^2\, C(\mathsf{z})\Delta z,
\end{aligned}$$

where the third equality holds because of the Proposition 1. □

Proposition 3 *For the cubic spline based semi-Lagrangian scheme (12) with an infinite domain $\mathbb{R}$ and uniform grids $\mathbb{G}^z$, we have*

$$\sum_{\mathsf{z}\in\mathbb{G}^z} \mathbf{f}_{\mathsf{z}}^{n+1}\, \mathsf{z}^s = \sum_{\mathsf{z}\in\mathbb{G}^z} \mathbf{f}_{\mathsf{z}}^{n}\, (\mathsf{z}+c\Delta t)^s, \quad s = 0, 1, 2.$$

Proof For the cubic spline interpolation of $\mathbf{f}^n$, $\mathcal{I}\mathbf{f}^n(z) = \sum_{z\in\mathbb{G}^z} \mathbf{e}_z N(z-\mathsf{z})$, we have $\mathbf{f}_{\mathsf{z}}^n = \mathcal{I}\mathbf{f}^n(\mathsf{z})$, and $\mathbf{f}_{\mathsf{z}}^{n+1} = \mathcal{I}\mathbf{f}^n(\mathsf{z} - c\Delta t)$. Then we have

$$\begin{aligned}
\sum_{\mathsf{z}\in\mathbb{G}^z} \mathbf{f}_{\mathsf{z}}^{n+1}\, \mathsf{z}^s &= \sum_{\mathsf{z}\in\mathbb{G}^z} \sum_{\tilde{\mathsf{z}}\in\mathbb{G}^z} \mathbf{e}_{\tilde{\mathsf{z}}}\, C(\mathsf{z}-\tilde{\mathsf{z}}-c\Delta t)\, \mathsf{z}^s = \sum_{\mathsf{z}\in\mathbb{G}^z} \sum_{\tilde{\mathsf{z}}\in\mathbb{G}^z} \mathbf{e}_{\tilde{\mathsf{z}}}\, C(\mathsf{z}-\tilde{\mathsf{z}})\, (\mathsf{z}+c\Delta t)^s \\
&= \sum_{\mathsf{z}\in\mathbb{G}^z} \mathbf{f}_{\mathsf{z}}^{n}\, (\mathsf{z}+c\Delta t)^s,
\end{aligned}$$

where for each $\tilde{\mathsf{z}}$, we have used the Proposition 2. □

Next we give three identities of the scheme (12), which will be used in the following for proving the conservation properties of the schemes.

Lemma 2 *For the cubic spline based semi-Lagrangian method* (12) *for the equation* (10) *with an infinite domain* $\mathbb{R}$ *and uniform grids* $\mathbb{G}^z$*, we have the following identities*

$$\sum_{\mathsf{z}\in\mathbb{G}^z} \mathbf{f}_{\mathsf{z}}^{n+1} = \sum_{\mathsf{z}\in\mathbb{G}^z} \mathbf{f}_{\mathsf{z}}^{n}, \quad \sum_{\mathsf{z}\in\mathbb{G}^z} \mathsf{z}\,\mathbf{f}_{\mathsf{z}}^{n+1} = \sum_{\mathsf{z}\in\mathbb{G}^z} \mathsf{z}\,\mathbf{f}_{\mathsf{z}}^{n} + c\,\Delta t \sum_{\mathsf{z}\in\mathbb{G}^z} \mathbf{f}_{\mathsf{z}}^{n},$$
$$\frac{1}{2}\sum_{\mathsf{z}\in\mathbb{G}^z} \mathsf{z}^2\,\mathbf{f}_{\mathsf{z}}^{n+1} = \frac{1}{2}\sum_{\mathsf{z}\in\mathbb{G}^z} \mathsf{z}^2\,\mathbf{f}_{\mathsf{z}}^{n} + c\,\Delta t\left(\sum_{\mathsf{z}\in\mathbb{G}^z} \mathsf{z}\,\mathbf{f}_{\mathsf{z}}^{n} + \frac{c\Delta t}{2}\sum_{\mathsf{z}\in\mathbb{G}^z} \mathbf{f}_{\mathsf{z}}^{n}\right).$$

Proof The first two equalities have already been proved in the Proposition 14 and 15 in [37]. Here we focus on the third equality, which can be proved with Proposition 3 and has been mentioned in [37]. For the cubic spline interpolation of $\mathbf{f}^n$, $\mathcal{I}\mathbf{f}^n(z) = \sum_{\mathsf{z}\in\mathbb{G}^z} \mathbf{e}_{\mathsf{z}} C(z-\mathsf{z})$, we have $\mathbf{f}_{\mathsf{z}}^n = \mathcal{I}\mathbf{f}^n(\mathsf{z})$, and $\mathbf{f}_{\mathsf{z}}^{n+1} = \mathcal{I}\mathbf{f}^n(\mathsf{z} - c\Delta t)$. With the Proposition 3, we have

$$\begin{aligned}\frac{1}{2}\sum_{\mathsf{z}\in\mathbb{G}^z} \mathsf{z}^2\,\mathbf{f}_{\mathsf{z}}^{n+1} &= \frac{1}{2}\sum_{\mathsf{z}\in\mathbb{G}^z} (\mathsf{z}+c\Delta t)^2\mathbf{f}_{\mathsf{z}}^{n}\\ &= \frac{1}{2}\sum_{\mathsf{z}\in\mathbb{G}^z} \mathsf{z}^2\,\mathbf{f}_{\mathsf{z}}^{n} + \frac{1}{2}\sum_{\mathsf{z}\in\mathbb{G}^z} c^2\Delta t^2\mathbf{f}_{\mathsf{z}}^{n} + c\,\Delta t\sum_{\mathsf{z}\in\mathbb{G}^z} \mathsf{z}\,\mathbf{f}_{\mathsf{z}}^{n}.\end{aligned}$$

Thus we have finished the proof. □

Remark 1 In practical simulations, the infinite velocity domain is truncated to a sufficient large finite domain, such that the distribution functions are very small near the boundaries, which makes the Proposition 2-3 hold with round-off errors for the first and second order moments [37].

4 Sub-Steps

Here, we present the discretization for sub-steps pvb and xv. After full discretization, we have the following discrete mass $\mathcal{M}_h$, α-th component of momentum $\mathcal{P}_{h,\alpha}$, and energy $\mathcal{E}_h$, the conservation of which will be considered for each sub-step,

$$\begin{aligned}\mathcal{M}_h &= \sum_{\mathsf{xv}} \mathbf{f}_{\mathsf{xv}}\,\Delta\boldsymbol{x}\,\Delta\boldsymbol{v}, \quad \mathcal{P}_{h,\alpha} = \sum_{\mathsf{xv}} \mathsf{v}_\alpha\mathbf{f}_{\mathsf{xv}}\,\Delta\boldsymbol{x}\,\Delta\boldsymbol{v},\\ \mathcal{E}_h &= \frac{1}{2}\sum_{\mathsf{xv}} |\mathsf{v}|^2\mathbf{f}_{\mathsf{xv}}\,\Delta\boldsymbol{x}\,\Delta\boldsymbol{v} + \frac{1}{2}\sum_{\mathsf{x}} |\mathbf{B}_{\mathsf{x}}|^2\,\Delta\boldsymbol{x} + \frac{1}{\gamma-1}\sum_{\mathsf{x}} \mathbf{p}_{\mathsf{x}}\,\Delta\boldsymbol{x}\\ &=: K_{f,h} + K_{B,h} + K_{p,h}.\end{aligned} \tag{13}$$

As mentioned in Remark 1, in this section we work with a periodic boundary condition in space and an infinite velocity domain, and in the practical simulations we have to truncate the velocity domain into a sufficiently large finite velocity domain, which makes the conservation properties of the momentum and energy we prove in this section hold with round off errors [37].

4.1 Sub-Step *pvb*

The equation of this sub-step is

$$\begin{aligned}
&\frac{\partial f}{\partial t} + (\boldsymbol{E} + \boldsymbol{v} \times \boldsymbol{B}) \cdot \frac{\partial f}{\partial \boldsymbol{v}} = 0\,,\\
&\frac{\partial \boldsymbol{B}}{\partial t} = -\nabla \times \boldsymbol{E}, \quad \boldsymbol{E} = -\frac{\nabla p}{\rho} - \boldsymbol{u}_{\mathrm{e}} \times \boldsymbol{B},\\
&\frac{\partial p}{\partial t} + \nabla \cdot (\boldsymbol{u}_{\mathrm{e}}\, p) + (\gamma - 1)\, p\, \nabla \cdot \boldsymbol{u}_{\mathrm{e}} = 0, \quad \boldsymbol{u}_{\mathrm{e}} = \boldsymbol{u} - \frac{\boldsymbol{J}}{\rho}, \quad \gamma \neq 1,\\
&\frac{\partial \boldsymbol{u}}{\partial t} - (\boldsymbol{E} + \boldsymbol{u} \times \boldsymbol{B}) = 0,
\end{aligned} \tag{14}$$

where we include the equation of $\boldsymbol{u}$ by taking the velocity moments from the Vlasov equation

Time discretization. The following modified mid-point rule is used for the time discretization of (14) between the time interval $[t^n, t^{n+1}]$

$$\begin{aligned}
&\frac{\partial f}{\partial t} + \left(\boldsymbol{v} - \bar{\boldsymbol{u}} + \frac{\nabla \times \boldsymbol{B}^{n+\frac{1}{2}}}{\rho}\right) \times \boldsymbol{B}^{n+\frac{1}{2}} \cdot \frac{\partial f}{\partial \boldsymbol{v}} - \frac{\nabla p^{n+\frac{1}{2}}}{\rho} \cdot \frac{\partial f}{\partial \boldsymbol{v}} = 0,\\
&\frac{\boldsymbol{B}^{n+1} - \boldsymbol{B}^n}{\Delta t} = -\nabla \times \left(-\frac{\nabla p^{n+\frac{1}{2}}}{\rho} - \bar{\boldsymbol{u}}_{\mathrm{e}} \times \boldsymbol{B}^{n+\frac{1}{2}}\right),\\
&\frac{p^{n+1} - p^n}{\Delta t} + \nabla \cdot \left(p^{n+\frac{1}{2}} \bar{\boldsymbol{u}}_{\mathrm{e}}\right) + (\gamma - 1) p^{n+\frac{1}{2}}\, \nabla \cdot \bar{\boldsymbol{u}}_{\mathrm{e}} = 0, \ \bar{\boldsymbol{u}}_{\mathrm{e}} = \bar{\boldsymbol{u}} - \frac{\nabla \times \boldsymbol{B}^{n+\frac{1}{2}}}{\rho},\\
&\frac{\partial \boldsymbol{u}}{\partial t} - \left(\boldsymbol{u} - \bar{\boldsymbol{u}} + \frac{\nabla \times \boldsymbol{B}^{n+\frac{1}{2}}}{\rho}\right) \times \boldsymbol{B}^{n+\frac{1}{2}} + \frac{\nabla p^{n+\frac{1}{2}}}{\rho} = 0,
\end{aligned} \tag{15a}$$

$$\bar{\boldsymbol{u}} = \frac{1}{\Delta t} \int_{t^n}^{t^{n+1}} \boldsymbol{u}(t)\, \mathrm{d}t, \tag{15b}$$

in which f is not discretized in time and updated as

$$f(t^{n+1}, \boldsymbol{x}, \boldsymbol{v}) = f(t^n, \boldsymbol{x}, \boldsymbol{v}^n), \tag{16}$$

where $\boldsymbol{v}^n$ is the solution of the following characteristics at time t^n with $\boldsymbol{v}(t^{n+1}) = \boldsymbol{v}$,

$$\dot{\boldsymbol{v}} = \left(\boldsymbol{v} - \bar{\boldsymbol{u}} + \frac{\nabla \times \boldsymbol{B}^{n+\frac{1}{2}}}{\rho}\right) \times \boldsymbol{B}^{n+\frac{1}{2}} - \frac{\nabla p^{n+\frac{1}{2}}}{\rho}.$$

Also the equation of $\boldsymbol{u}$ (15a) [31, 37] is not discretized in time, and it can be solved with an explicit formula (18) given below. The density ρ is not changing in time, so we omit the time index. The $\bar{\boldsymbol{u}}$ is fixed by the condition (15b), i.e., $\bar{\boldsymbol{u}}$ is the time average of $\boldsymbol{u}(t)$ satisfying the equation (15a), which is obtained by the velocity moment of the Vlasov equation in (15).

To avoid the heavy iterations involving the kinetic part in implicit schemes, semi-implicit schemes [21, 25, 31] have been proposed, in which once the moment equations are derived and substituted into the field equations, the lower-dimensional field equations remain implicit, while the kinetic equations become explicit. Here we adopt a similar strategy, firstly derive the equation (15a) of $\boldsymbol{u}$, and then plug the $\bar{\boldsymbol{u}}$ obtained by solving (15a)-(15b) into the equations of $\boldsymbol{B}$ and p in (15). After solving field equations and obtaining the updated $\boldsymbol{B}$ and p, we finally solve the Vlasov equation. f is not involved in the iterations in the implicit scheme (15).

The $\bar{\boldsymbol{u}}$ determined by the condition (15b) is essential for preserving the scheme's conservation and cancellation-free properties, and it also removes the time dependence of $\boldsymbol{u}$ in the Vlasov equation, thereby enabling the use of the shifted-velocity-frame exact splitting introduced below, which avoids costly three-dimensional interpolations when applying semi-Lagrangian methods [38].

The explicit formula of $\bar{\boldsymbol{u}}$. By splitting $\frac{\nabla p^{n+\frac{1}{2}}}{\rho}$ into the parallel and perpendicular parts of the magnetic field, i.e., when $\boldsymbol{B}^{n+\frac{1}{2}} \neq 0$,

$$\begin{aligned} &\frac{\nabla p^{n+\frac{1}{2}}}{\rho} = \boldsymbol{q} \times \boldsymbol{B}^{n+\frac{1}{2}} + \left(\frac{\nabla p^{n+\frac{1}{2}}}{\rho}\right)_{\parallel}, \quad \boldsymbol{q} = \frac{\boldsymbol{B}^{n+\frac{1}{2}}}{|\boldsymbol{B}^{n+\frac{1}{2}}|^2} \times \frac{\nabla p^{n+\frac{1}{2}}}{\rho}, \\ &\left(\frac{\nabla p^{n+\frac{1}{2}}}{\rho}\right)_{\parallel} = \frac{\nabla p^{n+\frac{1}{2}} \cdot \boldsymbol{B}^{n+\frac{1}{2}}}{\rho} \frac{\boldsymbol{B}^{n+\frac{1}{2}}}{|\boldsymbol{B}^{n+\frac{1}{2}}|^2}, \end{aligned} \tag{17}$$

and when $\boldsymbol{B}^{n+\frac{1}{2}} = 0$, we set $\boldsymbol{q} = 0$ and regard $\frac{\nabla p^{n+\frac{1}{2}}}{\rho}$ parallel to $\boldsymbol{B}^{n+\frac{1}{2}}$, we have the solution of (15a)

$$\begin{aligned} \boldsymbol{u}(t) = e^{(t-t^n)\hat{\boldsymbol{B}}^{n+\frac{1}{2}}} &\left(\boldsymbol{u}^n - \bar{\boldsymbol{u}} + \frac{\nabla \times \boldsymbol{B}^{n+\frac{1}{2}}}{\rho} - \boldsymbol{q}\right) \\ &+ \bar{\boldsymbol{u}} - \frac{\nabla \times \boldsymbol{B}^{n+\frac{1}{2}}}{\rho} + \boldsymbol{q} - (t-t^n)\left(\frac{\nabla p^{n+\frac{1}{2}}}{\rho}\right)_{\parallel}, \end{aligned} \tag{18}$$

where $\hat{\boldsymbol{B}}\boldsymbol{v} := \boldsymbol{v} \times \boldsymbol{B}$. With the explicit formula of $e^{t\hat{\boldsymbol{B}}^{n+\frac{1}{2}}}$ [18]

$$e^{t\hat{\boldsymbol{B}}^{n+\frac{1}{2}}} = \mathbb{I}_3 + \frac{\sin(t|\boldsymbol{B}^{n+\frac{1}{2}}|)}{|\boldsymbol{B}^{n+\frac{1}{2}}|}\hat{\boldsymbol{B}}^{n+\frac{1}{2}} + 2\frac{\sin^2(\frac{t}{2}|\boldsymbol{B}^{n+\frac{1}{2}}|)}{|\boldsymbol{B}^{n+\frac{1}{2}}|^2}\hat{\boldsymbol{B}}^{n+\frac{1}{2}}\hat{\boldsymbol{B}}^{n+\frac{1}{2}}$$

and by directly calculating $\int_{t^n}^{t^{n+1}} \boldsymbol{u}(t)\,\mathrm{d}t$, we have the following explicit formula of $\bar{\boldsymbol{u}}$,

$$\bar{\boldsymbol{u}} = \boldsymbol{u}^n + \frac{\nabla \times \boldsymbol{B}^{n+\frac{1}{2}}}{\rho} - \boldsymbol{q} + \boldsymbol{M}^{-1}\left(-\frac{\nabla \times \boldsymbol{B}^{n+\frac{1}{2}}}{\rho} + \boldsymbol{q} - \frac{\Delta t}{2}\left(\frac{\nabla p^{n+\frac{1}{2}}}{\rho}\right)_{\parallel}\right), \tag{19}$$

where $\boldsymbol{M} = \frac{1}{\Delta t}\int_0^{\Delta t} e^{\tau\hat{\boldsymbol{B}}^{n+\frac{1}{2}}}\,\mathrm{d}\tau$.

Proposition 4 *The matrix $\boldsymbol{M}$ is invertible if $\Delta t|\boldsymbol{B}^{n+\frac{1}{2}}| \neq 2k\pi, k \in \mathbb{Z}, k \geq 1$.*

Proof The eigenvalues of $\hat{\boldsymbol{B}}^{n+\frac{1}{2}}$ are 0 and $\pm\mathrm{i}|\boldsymbol{B}^{n+\frac{1}{2}}|$, from which we know the eigenvalues of $\boldsymbol{M}$ are 1 and $\frac{\sin\theta}{\theta} \pm \mathrm{i}\frac{2}{\theta}\sin^2\left(\frac{\theta}{2}\right)$, where $\theta = \Delta t|\boldsymbol{B}^{n+\frac{1}{2}}|$. Then when $\theta \neq 2k\pi, k \in \mathbb{Z}, k \geq 1$, the eigenvalues of matrix $\boldsymbol{M}$ are non-zero, and matrix $\boldsymbol{M}$ is invertible. □

The Proposition 4 implies that the Δt used for solving the Vlasov equation in velocity should not be $2k\pi/|\boldsymbol{B}^{n+\frac{1}{2}}|$ with $k \in \mathbb{Z}, k \geq 1$.

As the time integral average approximates the mid-point value with the error of $\mathcal{O}(\Delta t^2)$, by comparing it with the standard mid-point rule, we know that the modified mid-point rule (15) is second order in time.

Reversibility. Then we consider the reversibility [16] of the modified mid-point rule (15).

Theorem 1 *The scheme* (15) *is reversible.*

Proof By the definition of reversible schemes, we need to prove when we exchange the unknowns at t^n with t^{n+1}, and set $\Delta t = -\Delta t$, the same scheme as (15) is obtained.

For the scheme of the magnetic field and pressure in (15), we can see we only need to prove $\bar{\boldsymbol{u}}$ is not changed when we exchange $\boldsymbol{u}^n$ with $\boldsymbol{u}^{n+1}$ and set $\Delta t = -\Delta t$, which is true due to the equation (15a) satisfied by $\boldsymbol{u}$ is reversible. Also the scheme of f is reversible, due to reversibility of the Vlasov equation in (15). □

Theorem 2 *When we assume a periodic boundary condition in space, and an infinite velocity domain, mass, momentum, and energy are conserved by the time discretization* (15). *Also the cancellation problem* (8) *is overcome.*

Proof The mass conservation is easy to prove by directly integrating the Vlasov equation in (15) in phase-space with the periodic boundary condition.

Multiplying by $\boldsymbol{v}$ on both sides of the Vlasov equation in (15) and then integrating with respect to $\boldsymbol{v}$ and t gives

$$\begin{aligned}\boldsymbol{J}_f^{n+1} - \boldsymbol{J}_f^n = \int_{t^n}^{t^{n+1}} \boldsymbol{J}_f(t) \times \boldsymbol{B}^{n+\frac{1}{2}} \,\mathrm{d}t - \Delta t\, \rho \bar{\boldsymbol{u}} \times \boldsymbol{B}^{n+\frac{1}{2}} \\ + \Delta t\, \nabla \times \boldsymbol{B}^{n+\frac{1}{2}} \times \boldsymbol{B}^{n+\frac{1}{2}} - \Delta t\, \nabla p^{n+\frac{1}{2}},\end{aligned} \tag{20}$$

where the first two terms cancel out due to the condition (15b), and thus the cancellation problem (8) is overcome. By integrating the above identity (20) with respect to $\boldsymbol{x}$, we get

$$\begin{aligned}\mathcal{P}^{n+1} - \mathcal{P}^n &= \int \left[\Delta t\, \nabla \times \boldsymbol{B}^{n+\frac{1}{2}} \times \boldsymbol{B}^{n+\frac{1}{2}} - \Delta t\, \nabla p^{n+\frac{1}{2}}\right] \mathrm{d}\boldsymbol{x} \\ &= \int \left[\Delta t\, \nabla \cdot \left(\boldsymbol{B}^{n+\frac{1}{2}} \boldsymbol{B}^{n+\frac{1}{2}} - \frac{|\boldsymbol{B}^{n+\frac{1}{2}}|^2}{2} \mathbb{I}_3\right) - \Delta t\, \nabla p^{n+\frac{1}{2}}\right] \mathrm{d}\boldsymbol{x} = 0,\end{aligned} \tag{21}$$

where in the second last equality we have used the condition $\nabla \cdot \boldsymbol{B}^{n+\frac{1}{2}} = 0$. This proves the momentum conservation.

Multiplying by $\frac{|\boldsymbol{v}|^2}{2}$ on both sides of the Vlasov equation in (15) and then integrating in phase-space and with respect to t between t^n and t^{n+1} gives

$$\begin{aligned}K_f^{n+1} - K_f^n = \int -\bar{\boldsymbol{u}} \times \boldsymbol{B}^{n+\frac{1}{2}} \cdot \boldsymbol{J}_f \,\mathrm{d}\boldsymbol{x}\,\mathrm{d}t \underbrace{- \int \frac{\nabla p^{n+\frac{1}{2}}}{\rho} \cdot \boldsymbol{J}_f \,\mathrm{d}\boldsymbol{x}\,\mathrm{d}t}_{a} \\ + \underbrace{\int \int \frac{\nabla \times \boldsymbol{B}^{n+\frac{1}{2}}}{\rho} \times \boldsymbol{B}^{n+\frac{1}{2}} \cdot \boldsymbol{J}_f \,\mathrm{d}\boldsymbol{x}\,\mathrm{d}t}_{b},\end{aligned} \tag{22}$$

where the first term vanishes due to the condition (15b). Multiplying by $\boldsymbol{B}^{n+\frac{1}{2}}$ on both sides of the equation for the magnetic field in (15) and then integrating with respect to $\boldsymbol{x}$ gives

$$\begin{aligned}K_B^{n+1} - K_B^n = -\Delta t \int \boldsymbol{B}^{n+\frac{1}{2}} \cdot \nabla \times \left(\frac{\nabla \times \boldsymbol{B}^{n+\frac{1}{2}}}{\rho} \times \boldsymbol{B}^{n+\frac{1}{2}}\right) \mathrm{d}\boldsymbol{x} \\ + \underbrace{\Delta t \int \boldsymbol{B}^{n+\frac{1}{2}} \cdot \nabla \times \left(\bar{\boldsymbol{u}} \times \boldsymbol{B}^{n+\frac{1}{2}}\right) \mathrm{d}\boldsymbol{x}}_{b} + \underbrace{\Delta t \int \boldsymbol{B}^{n+\frac{1}{2}} \cdot \nabla \times \frac{\nabla p^{n+\frac{1}{2}}}{\rho} \mathrm{d}\boldsymbol{x}}_{c},\end{aligned}$$

where the first term vanishes via integration by parts. Integrating the pressure equation in (15) with respect to $\boldsymbol{x}$ gives

$$K_p^{n+1} - K_p^n = \frac{-\Delta t}{\gamma - 1} \int \nabla \cdot (p^{n+\frac{1}{2}} \bar{\boldsymbol{u}}_e)\, \mathrm{d}\boldsymbol{x} \underbrace{-\Delta t \int p^{n+\frac{1}{2}} \nabla \cdot \bar{\boldsymbol{u}}\, \mathrm{d}\boldsymbol{x}}_{a} + \underbrace{\Delta t \int p^{n+\frac{1}{2}} \nabla \cdot \frac{\nabla \times \boldsymbol{B}^{n+\frac{1}{2}}}{\rho}\, \mathrm{d}\boldsymbol{x}}_{c},$$

where the first term vanishes via integration by parts. The sum of the remaining terms with the same label cancel out via integration by parts and the condition (15b), and the energy conservation is proved. □

Exact splitting. For the resolution of the distribution function, if we directly use semi-Lagrangian method [38] to solve (16), costly three dimensional interpolations are needed [28]. According to the theory in [3], exact splitting that avoids high dimensional interpolations can be constructed for (16). In the following, we give an explicit exact splitting for (16) with the help of the decomposition of the pressure term (17) and the exact splitting for rotations [3, 5]. With the exact splitting presented below, only one dimensional advections and interpolations are needed, and are thus efficient.

We firstly have a closer look at the characteristics,

$$\begin{aligned} \dot{\boldsymbol{v}} &= \left(\boldsymbol{v} - \bar{\boldsymbol{u}} - \boldsymbol{q} + \frac{\nabla \times \boldsymbol{B}^{n+\frac{1}{2}}}{\rho}\right) \times \boldsymbol{B}^{n+\frac{1}{2}} - \left(\frac{\nabla p^{n+\frac{1}{2}}}{\rho}\right)_{\parallel} \\ &=: \hat{\boldsymbol{B}}^{n+\frac{1}{2}} \left(\boldsymbol{v} - \bar{\boldsymbol{u}} - \boldsymbol{q} + \frac{\nabla \times \boldsymbol{B}^{n+\frac{1}{2}}}{\rho}\right) - \left(\frac{\nabla p^{n+\frac{1}{2}}}{\rho}\right)_{\parallel}, \end{aligned} \tag{23}$$

which defines the matrix $\hat{\boldsymbol{B}}^{n+\frac{1}{2}}$. The solution of this equation for $\boldsymbol{v}(t^n) = \boldsymbol{v}^n$ is

$$\boldsymbol{v}(t) = e^{(t-t^n)\hat{\boldsymbol{B}}^{n+\frac{1}{2}}} \left(\boldsymbol{v}^n - \bar{\boldsymbol{u}} - \boldsymbol{q} + \frac{\nabla \times \boldsymbol{B}^{n+\frac{1}{2}}}{\rho}\right) + \bar{\boldsymbol{u}} + \boldsymbol{q} - \frac{\nabla \times \boldsymbol{B}^{n+\frac{1}{2}}}{\rho} - (t - t^n) \left(\frac{\nabla p^{n+\frac{1}{2}}}{\rho}\right)_{\parallel}.$$

The rotation matrix $e^{(t-t^n)\hat{\boldsymbol{B}}^{n+\frac{1}{2}}}$ can be decomposed as the product of four shear matrices [3, 5, 8, 47]. Correspondingly, the distribution function can be solved via several one dimensional translations. Specifically, the distribution function can be updated as follows,

1. One dimensional advections in the three velocity directions.

$$f^n(\boldsymbol{v}) \to f^n \left(\boldsymbol{v} + \Delta t \left(\frac{\nabla p^{n+\frac{1}{2}}}{\rho}\right)_{\parallel}\right) =: f_1^n(\boldsymbol{v}) \tag{24}$$

.

2. One dimensional advections in the three velocity directions.

$$f_1^n(\boldsymbol{v}) \to f_1^n \left(\boldsymbol{v} + \bar{\boldsymbol{u}} + \boldsymbol{q} - \frac{\nabla \times \boldsymbol{B}^{n+\frac{1}{2}}}{\rho}\right) =: f_2^n(\boldsymbol{v}). \tag{25}$$

3. Solve the equation $\frac{\partial f}{\partial t} + (\boldsymbol{v} \times \boldsymbol{B}^{n+\frac{1}{2}}) \cdot \frac{\partial f}{\partial \boldsymbol{v}} = 0$ by exact splittings proposed in [3–5], i.e,

$$f_3^n(\boldsymbol{v}) = e^{-\Delta t \hat{\boldsymbol{B}}^{n+\frac{1}{2}} \boldsymbol{v} \cdot \nabla_v} f_2^n(\boldsymbol{v}) = e^{\Delta t y^{(l)} \cdot \boldsymbol{v}\, \partial_{v_s}} \Pi_{k,k\neq s} e^{\Delta t y^{(k)} \cdot \boldsymbol{v}\, \partial_{v_k}} e^{\Delta t y^{(r)} \cdot \boldsymbol{v}\, \partial_{v_s}} f_2^n(\boldsymbol{v}), \tag{26}$$

where s is any fixed number in $\{1, 2, 3\}$, $y_s^{(l)} = y_s^{(r)} = 0$, for $\forall k \neq s$, $y_k^{(k)} = 0$, $k \in \{1, 2, 3\}$, and $y^{(l)}, y^{(r)}, y^{(k)} \in \mathbb{R}^3$ can be obtained by an iterative method given in [5]. f_3^n is obtained from f_2^n in four steps, where in each step only one dimensional advections are needed.

4. One dimensional advections in the three velocity directions.

$$f_3^n(\boldsymbol{v}) \to f_3^n\left(\boldsymbol{v} - \bar{\boldsymbol{u}} - \boldsymbol{q} + \frac{\nabla \times \boldsymbol{B}^{n+\frac{1}{2}}}{\rho}\right) =: f^{n+1}(\boldsymbol{v}, t). \tag{27}$$

Remark 2 When we update the distribution function via one dimensional advections, we can also compute the second, third and fourth steps (25)-(27), and then compute the first step (24), i.e., (24) is commutative with (25)-(27). The reason can be seen from the solution of the characteristics (23). The term $-\Delta t \left(\nabla p^{n+\frac{1}{2}}/\rho\right)_{\|}$ is parallel to the magnetic field, and we have the following equivalent solution of the characteristics (23)

$$\boldsymbol{v}(t) = e^{(t-t^n)\hat{\boldsymbol{B}}^{n+\frac{1}{2}}} \left(\boldsymbol{v}^n - \bar{\boldsymbol{u}} - \boldsymbol{q} + \frac{\nabla \times \boldsymbol{B}^{n+\frac{1}{2}}}{\rho} - (t - t^n)\left(\frac{\nabla p^{n+\frac{1}{2}}}{\rho}\right)_{\|}\right) + \bar{\boldsymbol{u}} + \boldsymbol{q} - \frac{\nabla \times \boldsymbol{B}^{n+\frac{1}{2}}}{\rho}. \tag{28}$$

Remark 3 In practical simulations, as [34, 46] the second step (25) and last step (27) are equivalent to moving the velocity grids with

$$\mp\left(\bar{\boldsymbol{u}} + \boldsymbol{q} - \frac{\nabla \times \boldsymbol{B}^{n+\frac{1}{2}}}{\rho}\right).$$

And the step (26) is conducted with the new velocity grids after the second step. Exact splitting and moving velocity grids have been used in [34, 46], but the pressure term is not added in the exact splitting, also overcoming the cancellation problem and the conservation of momentum and energy have not been investigated.

Full discretization. We denote the above four steps (24)-(27) with the notations $\mathcal{T}_i, i = 0, 1, 2, 3$, respectively, in which the cubic spline based semi-Lagrangian methods [38] are used for the one dimensional translations, i.e.,

$$\mathbf{f}^{n+1} = \mathcal{T}_3\, \mathcal{T}_2\, \mathcal{T}_1\, \mathcal{T}_0\, \mathbf{f}^n.$$

And we use Fourier spectral method to discretize the magnetic field and pressure. Specifically, we have the following full discretization.

$$
\begin{aligned}
&\mathbf{f}^{n+1} = \mathcal{T}_3\,\mathcal{T}_2\,\mathcal{T}_1\,\mathcal{T}_0\,\mathbf{f}^n,\\
&\mathbf{B}^{n+1} = \mathbf{B}^n - \Delta t\,\nabla\times\left(-\bar{\mathbf{u}}_{\mathrm{e}}\times\mathbf{B}^{n+\frac{1}{2}} - \frac{\nabla\mathbf{p}^{n+\frac{1}{2}}}{\rho}\right),\\
&\frac{\mathbf{p}^{n+1}-\mathbf{p}^n}{\Delta t} + \nabla\cdot(\bar{\mathbf{u}}_e\mathbf{p}^{n+\frac{1}{2}}) + (\gamma-1)\,\mathbf{p}^{n+\frac{1}{2}}\,(\nabla\cdot\bar{\mathbf{u}}_e) = 0,\\
&\frac{\partial\mathbf{u}}{\partial t} - \left(\mathbf{u}-\bar{\mathbf{u}}+\frac{\nabla\times\mathbf{B}^{n+\frac{1}{2}}}{\rho}\right)\times\mathbf{B}^{n+\frac{1}{2}} + \frac{\nabla\mathbf{p}^{n+\frac{1}{2}}}{\rho} = 0, \qquad (29a)\\
&\bar{\mathbf{u}} = \frac{1}{\Delta t}\int_{t^n}^{t^{n+1}}\mathbf{u}(t)\,\mathrm{d}t, \qquad (29b)
\end{aligned}
$$

where $\bar{\mathbf{u}}_e = \bar{\mathbf{u}} - \frac{\nabla\times\mathbf{B}^{n+\frac{1}{2}}}{\rho}$. Similarly to the time semi-discretization (15), we have the explicit formula for $\bar{\mathbf{u}}$:

$$
\begin{aligned}
\bar{\mathbf{u}} = \mathbf{u}^n &+ \frac{\nabla\times\mathbf{B}^{n+\frac{1}{2}}}{\rho} - \mathbf{q}\\
&+ \mathbf{M}^{-1}\left(-\frac{\nabla\times\mathbf{B}^{n+\frac{1}{2}}}{\rho} + \mathbf{q} - \frac{\Delta t}{2}\left(\frac{\nabla\mathbf{p}^{n+\frac{1}{2}}}{\rho}\right)_{\parallel}\right),
\end{aligned} \qquad (30)
$$

where $\mathbf{M} = \frac{1}{\Delta t}\int_0^{\Delta t} e^{\tau\hat{\mathbf{B}}^{n+\frac{1}{2}}}\,\mathrm{d}\tau$. We denote the numerical solution map of sub-step pvb as ϕ^t_{pvb}.

Theorem 3 *When we assume a periodic boundary condition in space, and an infinite velocity domain, the mass, momentum, and energy* (13) *are conserved by the scheme* (29) *of sub-step pvb, the cancellation problem* (8) *is overcome, and the magnetic field obtained is divergence free.*

Proof From (29) we have

$$
\nabla\cdot\mathbf{B}^{n+1} = \nabla\cdot\mathbf{B}^n - \Delta t\,\nabla\cdot\nabla\times\left(-\bar{\mathbf{u}}_{\mathrm{e}}\times\mathbf{B}^{n+\frac{1}{2}} - \frac{\nabla\mathbf{p}^{n+\frac{1}{2}}}{\rho}\right)
$$

As $\nabla\cdot\nabla\times = 0$, we know that the magnetic field is divergence free provided it is initially.

The discrete mass, $\mathcal{M}_h^n$, is conserved, as the distribution function is updated by the one dimensional advections in (24)-(27), each of which conserves the mass due to the first identity in Proposition 2.

With Propositions 2 and 3, we get the following updated mean velocity corresponding to the four steps (24)-(27),

$$
\begin{aligned}
\mathbf{u}^{n,1} &= \mathbf{u}^n - \Delta t\left(\frac{\nabla\mathbf{p}^{n+\frac{1}{2}}}{\rho}\right)_{\parallel},\\
\mathbf{u}^{n,2} &= \mathbf{u}^{n,1} - \bar{\mathbf{u}} - \mathbf{q} + \frac{\nabla\times\mathbf{B}^{n+\frac{1}{2}}}{\rho},\\
\mathbf{u}^{n,3} &= e^{\Delta t\hat{\mathbf{B}}^{n+\frac{1}{2}}}\mathbf{u}^{n,2},
\end{aligned}
$$

$$\mathbf{u}^{n+1} = \mathbf{u}^{n,3} + \bar{\mathbf{u}} + \mathbf{q} - \frac{\nabla \times \mathbf{B}^{n+\frac{1}{2}}}{\rho}.$$

We can verify that $\mathbf{u}^{n+1}$ is the solution of the equation (29a) at $t = t^{n+1}$ with the condition $\mathbf{u}(t^n) = \mathbf{u}^n$. Then by integrating the equation (29a) we have

$$\mathbf{u}^{n+1} - \mathbf{u}^n = \int_{t^n}^{t^{n+1}} \left[\left(\mathbf{u} - \bar{\mathbf{u}} + \frac{\nabla \times \mathbf{B}^{n+\frac{1}{2}}}{\rho} \right) \times \mathbf{B}^{n+\frac{1}{2}} - \frac{\nabla \mathbf{p}^{n+\frac{1}{2}}}{\rho} \right] \mathrm{d}t,$$

where the first two terms cancel each other due to the condition (29b). Then we have

$$\mathbf{u}^{n+1} - \mathbf{u}^n = \Delta t \, \frac{\nabla \times \mathbf{B}^{n+\frac{1}{2}}}{\rho} \times \mathbf{B}^{n+\frac{1}{2}} - \Delta t \, \frac{\nabla \mathbf{p}^{n+\frac{1}{2}}}{\rho},$$

i.e., the cancellation problem (8) is overcome. Then we can calculate the momentum and get

$$\mathcal{P}_h^{n+1} - \mathcal{P}_h^n = \Delta t \, \Delta \boldsymbol{x} \sum_{\mathsf{x} \in \mathbb{G}^x} \left(\nabla \times \mathbf{B}^{n+\frac{1}{2}} \right)_{\mathsf{x}} \times \mathbf{B}_{\mathsf{x}}^{n+\frac{1}{2}} - \Delta t \, \Delta \boldsymbol{x} \sum_{\mathsf{x} \in \mathbb{G}^x} (\nabla \mathbf{p})_{\mathsf{x}},$$

where the second term is zero, as by the definition of the discrete Fourier transform, for the zeroth mode

$$\sum_{\mathsf{x} \in \mathbb{G}^x} (\nabla \mathbf{p})_{\mathsf{x}} = (\widehat{\nabla \mathbf{p}})_0 = 0 \, \mathrm{i} \, (\widehat{\mathbf{p}})_0 = 0. \tag{31}$$

As for the first term, with $\nabla \cdot \mathbf{B}^{n+\frac{1}{2}} = 0$, we have

$$\sum_{\mathsf{x} \in \mathbb{G}^x} \left(\nabla \times \mathbf{B}^{n+\frac{1}{2}} \right)_{\mathsf{x}} \times \mathbf{B}_{\mathsf{x}}^{n+\frac{1}{2}} = \sum_{\mathsf{x} \in \mathbb{G}^x} \left[\nabla \cdot \left(\boldsymbol{B}_h^{n+\frac{1}{2}} \boldsymbol{B}_h^{n+\frac{1}{2}} - \frac{|\boldsymbol{B}_h^{n+\frac{1}{2}}|^2}{2} \mathbb{I}_3 \right) \right] (\mathsf{x}), \tag{32}$$

where $\boldsymbol{B}_h$ is the trigonometric interpolating polynomial

$$\boldsymbol{B}_h(\boldsymbol{x}) = \sum_{\xi \in \hat{\mathbb{G}}^x} \hat{\mathbf{B}}_\xi e^{\mathrm{i}\xi \boldsymbol{x}}, \quad \text{with } \boldsymbol{B}_h(\mathsf{x}) = \mathbf{B}_{\mathsf{x}}.$$

By the discrete orthogonality of the Fourier basis [36], i.e.,

$$\sum_{\mathsf{x} \in \mathbb{G}^x} e^{\mathrm{i}\xi \mathsf{x}} e^{-\mathrm{i}\xi' \mathsf{x}} = M_1 M_2 M_3 \, \delta_{\xi, \xi'}, \quad \forall \xi, \xi' \in \hat{\mathbb{G}}^x,$$

we know Eq (32) is equal to zero. Then we have proved the momentum conservation.

We define the kinetic energy density as $k_{f,\mathsf{x}} = \frac{1}{2} \sum_{\mathsf{v}} |\mathsf{v}|^2 \mathbf{f}_{\mathsf{xv}} \, \Delta \boldsymbol{v}$. With Propositions 3 and 2, we get the following updated kinetic energy density corresponding to the four steps (24)-(27),

$$k_f^{n,1} = k_f^n - \Delta t \, \rho \left(\frac{\nabla \mathbf{p}^{n+\frac{1}{2}}}{\rho} \right)_{\parallel} \cdot \frac{\mathbf{u}^n + \mathbf{u}^{n,1}}{2}$$

$$k_f^{n,2} = k_f^{n,1} - \Delta t \, \rho \left(\bar{\mathbf{u}} + \mathbf{q} - \frac{\nabla \times \mathbf{B}^{n+\frac{1}{2}}}{\rho} \right) \cdot \frac{\mathbf{u}^{n,1} + \mathbf{u}^{n,2}}{2}$$

$$k_f^{n,3} = k_f^{n,2}$$

$$k_f^{n+1} = k_f^{n,3} + \Delta t \, \rho \left(\bar{\mathbf{u}} + \mathbf{q} - \frac{\nabla \times \mathbf{B}^{n+\frac{1}{2}}}{\rho} \right) \cdot \frac{\mathbf{u}^{n,3} + \mathbf{u}^{n+1}}{2}.$$

We can verify that k_f^{n+1} is the solution of the equation

$$\begin{aligned}\frac{\partial k_f}{\partial t} + \rho\bar{\mathbf{u}} \times \mathbf{B}^{n+\frac{1}{2}} \cdot \mathbf{u} - \rho\left(\frac{\nabla \times \mathbf{B}^{n+\frac{1}{2}}}{\rho} \times \mathbf{B}^{n+\frac{1}{2}}\right) \cdot \mathbf{u} \\ + \rho\frac{\nabla \mathbf{p}^{n+\frac{1}{2}}}{\rho} \cdot \mathbf{u} = 0,\end{aligned} \tag{33}$$

at $t = t^{n+1}$ with the condition $k_f(t^n) = k_f^n$, where the $\mathbf{u}$ in (33)is the solution of the equation (29a) with the condition $\mathbf{u}(t^n) = \mathbf{u}^n$. By integrating the equation (33) in time we have

$$\begin{aligned}k_f^{n+1} - k_f^n = -\int_{t^n}^{t^{n+1}} \rho\bar{\mathbf{u}} \times \mathbf{B}^{n+\frac{1}{2}} \cdot \mathbf{u}\, \mathrm{d}t \\ + \int_{t^n}^{t^{n+1}} \left[\rho\left(\frac{\nabla \times \mathbf{B}^{n+\frac{1}{2}}}{\rho} \times \mathbf{B}^{n+\frac{1}{2}}\right) \cdot \mathbf{u} - \rho\frac{\nabla \mathbf{p}^{n+\frac{1}{2}}}{\rho} \cdot \mathbf{u}\right] \mathrm{d}t,\end{aligned} \tag{34}$$

where the first term is zero due to the condition (29b). Then with the condition (29b), we have

$$k_f^{n+1} - k_f^n = \Delta t\, \rho\left(\frac{\nabla \times \mathbf{B}^{n+\frac{1}{2}}}{\rho} \times \mathbf{B}^{n+\frac{1}{2}}\right) \cdot \bar{\mathbf{u}} - \Delta t\rho\frac{\nabla \mathbf{p}_h^{n+\frac{1}{2}}}{\rho} \cdot \bar{\mathbf{u}}. \tag{35}$$

Summing the equation (35) over x and multiplying with $\Delta \boldsymbol{x}$ gives

$$\begin{aligned}K_{f,h}^{n+1} - K_{f,h}^n = \underbrace{\Delta t\, \Delta \boldsymbol{x} \sum_{\mathsf{x} \in \mathbb{G}^x} \rho_{\mathsf{x}} \left(\frac{(\nabla \times \mathbf{B}^{n+\frac{1}{2}})_{\mathsf{x}}}{\rho_{\mathsf{x}}} \times \mathbf{B}_{\mathsf{x}}^{n+\frac{1}{2}}\right) \cdot \bar{\mathbf{u}}_{\mathsf{x}}}_{a} \\ \underbrace{-\Delta t\, \Delta \boldsymbol{x} \sum_{\mathsf{x} \in \mathbb{G}^x} \rho_{\mathsf{x}} \frac{(\nabla \mathbf{p}^{n+\frac{1}{2}})_{\mathsf{x}}}{\rho_{\mathsf{x}}} \cdot \bar{\mathbf{u}}_{\mathsf{x}}}_{b}.\end{aligned} \tag{36}$$

Multiplying with $\mathbf{B}_{\mathsf{x}}^{n+\frac{1}{2}}$ on both sides of the second equation in (29) and summing with x, we have

$$\begin{aligned}K_{B,h}^{n+1} - K_{B,h}^n = \underbrace{\Delta t\, \Delta \boldsymbol{x} \sum_{\mathsf{x} \in \mathbb{G}^x} (\nabla \times \mathbf{B}^{n+\frac{1}{2}})_{\mathsf{x}} \cdot \left(\bar{\mathbf{u}}_{\mathsf{x}} \times \mathbf{B}_{\mathsf{x}}^{n+\frac{1}{2}}\right)}_{a} \\ - \Delta t\, \Delta \boldsymbol{x} \sum_{\mathsf{x} \in \mathbb{G}^x} (\nabla \times \mathbf{B}^{n+\frac{1}{2}})_{\mathsf{x}} \cdot \left(\frac{(\nabla \times \mathbf{B}^{n+\frac{1}{2}})_{\mathsf{x}}}{\rho_{\mathsf{x}}} \times \mathbf{B}_{\mathsf{x}}^{n+\frac{1}{2}}\right) \\ \underbrace{+ \Delta t\, \Delta \boldsymbol{x} \sum_{\mathsf{x} \in \mathbb{G}^x} (\nabla \times \mathbf{B}^{n+\frac{1}{2}})_{\mathsf{x}} \cdot \frac{(\nabla \mathbf{p}^{n+\frac{1}{2}})_{\mathsf{x}}}{\rho_{\mathsf{x}}}}_{c},\end{aligned}$$

where the second term is zero.

Summing the third equation in (29) gives

$$K_{p,h}^{n+1} - K_{p,h}^{n} = -\frac{1}{\gamma - 1}\Delta t\, \Delta \boldsymbol{x} \sum_{\mathsf{x}\in\mathbb{G}^x} \left(\nabla \times (\mathbf{u}_e^{n+\frac{1}{2}} \mathbf{p}^{n+\frac{1}{2}})\right)_{\mathsf{x}}$$
$$+ \underbrace{\Delta t\, \Delta \boldsymbol{x} \sum_{\mathsf{x}\in\mathbb{G}^x} (\nabla \mathbf{p}^{n+\frac{1}{2}})_{\mathsf{x}} \cdot \bar{\mathbf{u}}_{\mathsf{x}}^{n+\frac{1}{2}}}_{b} \underbrace{-\Delta t\, \Delta \boldsymbol{x} \sum_{\mathsf{x}\in\mathbb{G}^x} (\nabla \mathbf{p}^{n+\frac{1}{2}})_{\mathsf{x}} \cdot \frac{(\nabla \times \mathbf{B}^{n+\frac{1}{2}})_{\mathsf{x}}}{\boldsymbol{\rho}_{\mathsf{x}}}}_{c},$$

where the first term is zero. The remaining terms with the same label cancel with each other, and we have proved the energy conservation.

In conclusion, we have proved the mass, momentum, and energy conservation, the magnetic field is divergence free if it hold initially, also the cancellation problem (8) is overcome. □

Remark 4 Without destroying the conservation properties, the magnetic field and pressure can also be discretized using the central finite difference method, the important properties of which include $\nabla \times \nabla = 0$, $\nabla \cdot \nabla \times = 0$, and integration parts [39].

Remark 5 The scheme (29) is not reversible. The reason is that the cubic spline based semi-Lagrangian method for one dimensional advections is not reversible.

Remark 6 In the case of isothermal/adiabatic electrons, there is no pressure equation in the hybrid model, instead the pressure p is determined by the density ρ directly, i.e., $p = \kappa\rho$, and $p = \mathcal{C}\rho^{\gamma}$, respectively. Similar to theorem 3, the scheme (29) without the scheme of the pressure but with the relation $p = \kappa\rho^{\gamma}$ or $p = \mathcal{C}\rho^{\gamma}$ can be proved to preserve the mass and momentum. The energy, including a non-quadratic thermal energy term, is not conserved [27]. Also the magnetic field is divergence free if it is initially, and the cancellation problem (8) is overcome.

As a summary of the sub-step (14), we write the computation steps into Algorithm 4.1.

4.2 Sub-Step *xv*

The equation of this sub-step is

$$\frac{\partial f}{\partial t} = -\boldsymbol{v} \cdot \nabla_x f$$

for which only one dimensional translations need to be done, for which we choose to use the Fourier spectral method (11) in each spatial direction. We denote the numerical solution map of sub-step pxv as ϕ_{xv}^{t}.

Theorem 4 *When we assume a periodic boundary condition in space, the scheme* (11) *of sub-step* xv *conserves mass, momentum, and energy defined in* (13) *exactly.*

Proof We explicitly write out the scheme (11) for sub-step xv as

$$\mathbf{f}^{n+1} = \mathcal{F}_3^{-1}\mathcal{F}_2^{-1}\mathcal{F}_1^{-1}[-\mathrm{i}\,\Delta t \vee \xi \mathcal{F}_3\mathcal{F}_2\mathcal{F}_1\mathbf{f}^{n}],$$

from which we know $\hat{\mathbf{f}}_{0\mathsf{v}}^{n+1} = \hat{\mathbf{f}}_{0\mathsf{v}}^{n}$. The mass, α-component of momentum, and energy (13) can be denoted as

$$\sum_{\mathsf{x}\in\mathbb{G}^x} \sum_{\mathsf{v}\in\mathbb{G}^v} m(\mathsf{v})\, \mathbf{f}_{\mathsf{xv}}\, \Delta \boldsymbol{x}\, \Delta \boldsymbol{v},$$

Algorithm 1 Sub-step pvb, n-th step to $(n+1)$-th step

Input: $\mathbf{f}^n$, $\mathbf{B}^n$, $\mathbf{p}^n$
Compute $\boldsymbol{\rho}^n$, $\mathbf{u}^n$ with $\mathbf{f}^n$
Start Picard iteration with $\mathbf{B}^{n+1,0} = \mathbf{B}^n$, $\mathbf{p}^{n+1,0} = \mathbf{p}^n$
for $k = 0$ to Maximum Picard iteration number **do**
  Compute mid-point values, $\mathbf{B}^{n+\frac{1}{2},k} = \frac{\mathbf{B}^n + \mathbf{B}^{n+1,k}}{2}$, $\mathbf{p}^{n+\frac{1}{2},k} = \frac{\mathbf{p}^n + \mathbf{p}^{n+1,k}}{2}$
  Compute $\bar{\mathbf{u}}$ with $\mathbf{B}^{n+\frac{1}{2},k}$, $\mathbf{p}^{n+\frac{1}{2},k}$, and $\boldsymbol{\rho}^n$ by Eq. (30)
  Plug $\bar{\mathbf{u}}$ into the Eqs. (29a)-(29b) and update $\mathbf{B}^{n+1,k+1}$ and $\mathbf{p}^{n+1,k+1}$,

$$\mathbf{B}^{n+1,k+1} = \mathbf{B}^n + \Delta t \nabla \times \left(\bar{\mathbf{u}} \times \mathbf{B}^{n+\frac{1}{2},k} - \frac{\nabla \times \mathbf{B}^{n+\frac{1}{2},k}}{\boldsymbol{\rho}^n} \times \mathbf{B}^{n+\frac{1}{2},k} + \frac{\nabla \mathbf{p}^{n+\frac{1}{2},k}}{\boldsymbol{\rho}^n} \right)$$

$$\mathbf{p}^{n+1,k+1} = \mathbf{p}^n - \Delta t \nabla \cdot (\bar{\mathbf{u}}_e^k \mathbf{p}^{n+\frac{1}{2},k}) - \Delta t(\gamma - 1)\, \mathbf{p}^{n+\frac{1}{2},k} \left(\nabla \cdot \bar{\mathbf{u}}_e^k \right)$$

  where $\bar{\mathbf{u}}_e^k = \bar{\mathbf{u}} - \frac{\nabla \times \mathbf{B}^{n+\frac{1}{2},k}}{\boldsymbol{\rho}^n}$
  if $\|\mathbf{B}^{n+1,k} - \mathbf{B}^{n+1,k+1}\| + \|\mathbf{p}^{n+1,k} - \mathbf{p}^{n+1,k+1}\| <$ Tolerance **then**
    $\mathbf{B}^{n+1} = \mathbf{B}^{n+1,k+1}$, $\mathbf{p}^{n+1} = \mathbf{p}^{n+1,k+1}$, break
  end if
end for
Update $\mathbf{f}$ by $\mathbf{f}^{n+1} = \mathcal{T}_3 \mathcal{T}_2 \mathcal{T}_1 \mathcal{T}_0 \mathbf{f}^n$, with $\bar{\mathbf{u}}$, $\boldsymbol{\rho}^n$, $\mathbf{B}^{n+\frac{1}{2}}$, and $\mathbf{p}^{n+\frac{1}{2}}$
return $\mathbf{f}^{n+1}$, $\mathbf{B}^{n+1}$, $\mathbf{p}^{n+1}$

with $m(\mathsf{v}) = 1, \mathsf{v}_\alpha, |\mathsf{v}|^2/2$, respectively. Then we have

$$\begin{aligned} &\sum_{\mathsf{x}\in\mathbb{G}^x} \sum_{\mathsf{v}\in\mathbb{G}^v} m(\mathsf{v})\, \mathbf{f}_{\mathsf{xv}}^{n+1}\, \Delta \boldsymbol{x}\, \Delta \boldsymbol{v} = \sum_{\mathsf{v}\in\mathbb{G}^v} m(\mathsf{v})\, \hat{\mathbf{f}}_{0\mathsf{v}}^{n+1}\, \Delta \boldsymbol{x}\, \Delta \boldsymbol{v} \\ &= \sum_{\mathsf{v}\in\mathbb{G}^v} m(\mathsf{v})\, \hat{\mathbf{f}}_{0\mathsf{v}}^{n}\, \Delta \boldsymbol{x}\, \Delta \boldsymbol{v} = \sum_{\mathsf{x}\in\mathbb{G}^x} \sum_{\mathsf{v}\in\mathbb{G}^v} m(\mathsf{v})\, \mathbf{f}_{\mathsf{xv}}^{n}\, \Delta \boldsymbol{x}\, \Delta \boldsymbol{v}, \end{aligned} \tag{37}$$

i.e., the mass, momentum, and energy defined in (13) are conserved by the scheme (11). □

By the composition methods [16], we have the following second order Strang splitting method [41],

$$\phi_{xv}^{\frac{\Delta t}{2}}\, \phi_{pvb}^{\Delta t}\, \phi_{xv}^{\frac{\Delta t}{2}}.$$

5 1D-2V Reduced Model

Here, we consider a reduced model which is one dimensional in space and two dimensional in velocity, in which the distribution function is $f(t, x_1, v_1, v_2)$, and the magnetic field is in the form of $\boldsymbol{B} = (0, 0, B_3(x_1))^\top$. The reduced model reads

$$\begin{aligned} \frac{\partial f}{\partial t} &= -v_1 \frac{\partial f}{\partial x_1} - v_2 B_3 \frac{\partial f}{\partial v_1} + v_1 B_3 \frac{\partial f}{\partial v_2} + u_2 B_3 \frac{\partial f}{\partial v_1} - u_1 B_3 \frac{\partial f}{\partial v_2} \\ &\quad + \frac{1}{\rho} \frac{\partial p}{\partial x_1} \frac{\partial f}{\partial v_1} + \frac{1}{\rho} B_3 \frac{\partial B_3}{\partial x_1} \frac{\partial f}{\partial v_1} \\ \frac{\partial B_3}{\partial t} &= -\frac{\partial}{\partial x_1}(u_1 B_3), \quad \rho = \int f \,\mathrm{d}\boldsymbol{v}, \quad u_1 = \frac{1}{\rho} \int v_1 f \,\mathrm{d}\boldsymbol{v}, \quad u_2 = \frac{1}{\rho} \int v_2 f \,\mathrm{d}\boldsymbol{v}, \end{aligned}$$

$$\frac{\partial p}{\partial t}+\frac{\partial}{\partial x_1}\left(\frac{\int v_1 f\,\mathrm{d}\boldsymbol{v}}{\rho}p\right)+(\gamma-1)\,p\,\frac{\partial}{\partial x_1}\frac{\int v_1 f\,\mathrm{d}\boldsymbol{v}}{\rho}=0. \tag{38}$$

For this reduced model (38), we have the following two sub-steps after Poisson splitting [21, 27]. As in the three dimensional case, we use uniform grids in phase-space with grid numbers M_1, N_1, N_2 in directions x_1, v_1, v_2, respectively.

Sub-step pvb**.** The sub-step pvb is

$$\begin{aligned}
&\frac{\partial f}{\partial t}=-v_2B_3\frac{\partial f}{\partial v_1}+v_1B_3\frac{\partial f}{\partial v_2}+u_2B_3\frac{\partial f}{\partial v_1}-u_1B_3\frac{\partial f}{\partial v_2}\\
&\qquad+\frac{1}{\rho}\frac{\partial p}{\partial x_1}\frac{\partial f}{\partial v_1}+\frac{1}{\rho}B_3\frac{\partial B_3}{\partial x_1}\frac{\partial f}{\partial v_1}\\
&\frac{\partial B_3}{\partial t}=-\frac{\partial}{\partial x_1}(u_1B_3),\quad \rho=\int f\,\mathrm{d}\boldsymbol{v},\quad u_1=\frac{1}{\rho}\int v_1 f\,\mathrm{d}\boldsymbol{v},\quad u_2=\frac{1}{\rho}\int v_2 f\,\mathrm{d}\boldsymbol{v},\\
&\frac{\partial p}{\partial t}+\frac{\partial}{\partial x_1}\left(\frac{\int v_1 f\,\mathrm{d}\boldsymbol{v}}{\rho}p\right)+(\gamma-1)p\frac{\partial}{\partial x_1}\frac{\int v_1 f\,\mathrm{d}\boldsymbol{v}}{\rho}=0.
\end{aligned} \tag{39}$$

A scheme similar to (29) can be constructed, in which the two dimensional rotation is solved by the exact splitting presented in [4]. The scheme overcomes the cancellation problem, conserves mass, momentum, and energy.

Sub-step xv**.** The sub-step xv is

$$\frac{\partial f}{\partial t}=-v_1\frac{\partial f}{\partial x_1}. \tag{40}$$

This sub-step is solved with Fourier spectral method (11), and the mass, momentum, and energy are conserved.

6 Numerical Experiments

In this section, firstly we check the time accuracy order of the schemes constructed. Then we use the 1D-2V reduced model (38) to simulate Landau damping and Bernstein waves with the schemes constructed. The Fourier spectral method (11) is adopted for solving sub-step (40). And the cubic spline based semi-Lagrangian method (12) is used for solving the Vlasov equation in the sub-step (39). The tolerance of the Picard iteration is 10^{-14}.

6.1 Time Accuracy Order and Performance

Here we firstly check the time accuracy order by 1D-2V dimensional simulations. The initial conditions are:

$$f=\frac{1}{\pi v_T^2}(1+\delta\rho)e^{-\frac{|v_1-0.1|^2}{v_T^2}-\frac{|v_2-0.2|^2}{v_T^2}},$$

$$B_3=1+\sum_{k=1}^{8}0.01\sin(2kx_1),\quad p=0.09(1+\delta\rho)^{5/3},$$

where $\delta\rho=0.01\sin(2x_1)$, and $v_T=0.4$. The computational parameters are as follows, grid number $16\times128\times128$, and domain $[0,\pi]\times[-2.5,2.5]\times[-2.5,2.5]$. We use the Strang splitting $\phi_{xv}^{\frac{\Delta t}{2}}\phi_{pvb}^{\Delta t}\phi_{xv}^{\frac{\Delta t}{2}}$. In table 1, we present the l_1 error of f, B_3, and p at $t=0.1$,

Table 1 The l_1 errors and convergence orders of the unknowns for different time step sizes.

Δt	Error f	Order f	Error B_3	Order B_3	Error p	Order p
0.1	16.88	–	1.723×10^{-2}	–	2.611×10^{-3}	–
0.05	4.710	1.84	5.209×10^{-3}	1.73	7.884×10^{-4}	1.73
0.025	1.226	1.94	1.375×10^{-3}	1.92	2.081×10^{-4}	1.99
0.0125	0.3119	1.97	3.470×10^{-4}	1.99	5.252×10^{-5}	1.99
0.00625	0.0802	1.96	8.539×10^{-5}	2.02	1.292×10^{-5}	2.02

the reference solution is obtained by a very small time step 0.001. We can see when Δt becomes smaller, the order of convergence becomes closer to 2, which indicates that the Strang splitting gives a second order accuracy in time.

We check the performance of each part of the scheme for the above case with $\Delta t = 0.00625$. The field solver needs 6 Picard iterations to converge on average, the field solver takes 1.474×10^{-3}s per time step, the velocity advections with the cubic spline interpolation in the pvb sub-step take 0.198s per time step, the space advections by Fourier spectral method of sub-step xv take 0.157s per time step. Most of the computation time is spent on the kinetic part, because it has a higher dimensionality than the fields.

6.2 Landau Damping

Next we simulate ion Landau damping by 1D-2V dimensional simulations without background magnetic field. Initial conditions are:

$$f(x_1, v_1, v_2) = \frac{1}{\pi v_T^2}(1 + \delta\rho) e^{-\frac{|v_1|^2}{v_T^2} - \frac{|v_2|^2}{v_T^2}}, \quad B_3 = 0,$$

where $\delta\rho = 0.01 \sin(0.4x_1)$. Grid numbers are $32 \times 128 \times 64$, the simulation domain is $[0, 5\pi] \times [-8, 8] \times [-8, 8]$, the time step size is $\Delta t = 0.1$, and $v_T = 1.4142$. As there is not magnetic field, we regard the $\nabla p/\rho$ parallel to the magnetic field, and the steps (25)-(27) are not needed in ϕ^t_{pvb}. We used cubic splines interpolation for the velocity advections in sub-step pvb, and Fourier spectral method for the space advections in sub-stpe xv.

The numerical results with the Strang splitting $\phi_{xv}^{\frac{\Delta t}{2}} \phi_{pvb}^{\Delta t} \phi_{xv}^{\frac{\Delta t}{2}}$ [16] for the case of the isothermal electrons with $\kappa = 6.25$ are displayed in Fig. 1. As the pressure equation is not needed to solve in this case, the sub-step pvb is the usual semi-Lagrangian advection in velocity with the electron pressure gradient and no Picard iteration is needed. $\|\rho - 1\|_2^2$ with $\rho = \int f \, \mathrm{d}\boldsymbol{v}$ decays exponentially with a rate close to the theoretical one, which is obtained from the dispersion relation formula in [24, 39]. As semi-Lagrangian methods do not have noise, compared to the results of particle-in-cell method [27], a clear decay rate is observed. The energy error is around 10^{-6}. The mass error is around 10^{-14}, and momentum errors in v_1 and v_2 directions at the level of 10^{-14}, 10^{-17}, respectively.

Next we consider the case with the electron pressure equation and $\gamma = 5/3$. We use the Strang splitting $\phi_{xv}^{\frac{\Delta t}{2}} \phi_{pvb}^{\Delta t} \phi_{xv}^{\frac{\Delta t}{2}}$ [16]. The initial distribution function is the same as the isothermal electron case, and the initial electron pressure is $p(x_1) = 6.25/\gamma(1 + \delta\rho)^\gamma$. This case is equivalent to the formulation with adiabatic electrons $p = 6.25/\gamma(1 + \delta\rho)^\gamma$ and without explicitly using the pressure equation. The γ in the denominator of $p = 6.25/\gamma(1 + \delta\rho)^\gamma$

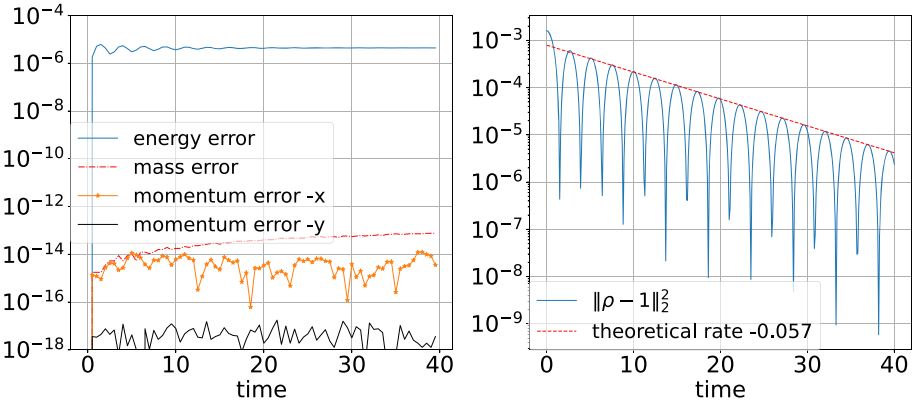

Fig. 1 **Landau damping** The formulation with the isothermal electrons. Time evolutions of energy error, mass error, momentum errors, and $\|\rho - 1\|_2^2$.

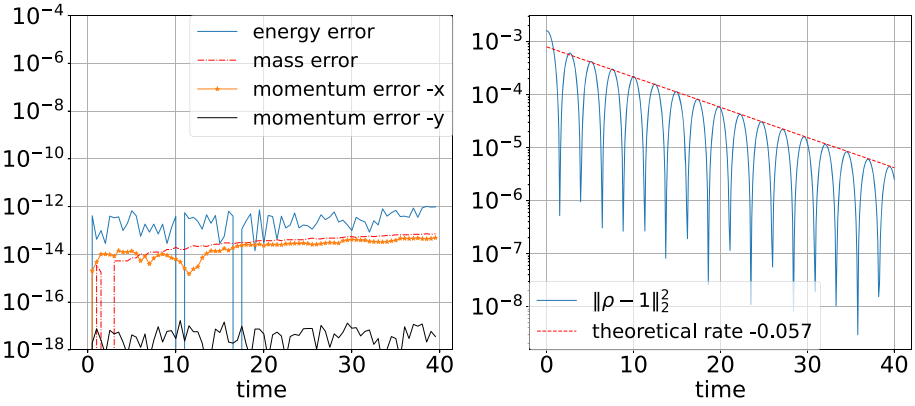

Fig. 2 **Landau damping** The formulation with the electron pressure equation. Time evolutions of energy error, mass error, momentum errors, and $\|\rho - 1\|_2^2$.

ensures that the linearized model coincides with the linearized isothermal case considered above, leading to the same decay rate for the perturbation of ρ. In the simulations, around 15 Picard iterations are used in the sub-step pvb. See the numerical results in Fig. 2. We can see the time evolution of $\|\rho - 1\|_2^2$ decays with the same rate as the isothermal electron case, mass error is around 10^{-14}, and momentum errors are 10^{-14}, 10^{-17} in x, y directions, respectively. The energy is also conserved very well, with an error around 10^{-12}.

6.3 Bernstein Waves

We use the 1D-2V reduced model for simulating the Bernstein waves. The initial conditions of the isothermal electron case are:

$$f(x_1, v_1, v_2) = \frac{1}{\pi v_T^2} e^{-\frac{|v_1|^2}{v_T^2} - \frac{|v_2|^2}{v_T^2}}, \quad B_3(x_1) = 1 + 10^{-5} \sum_{k=1}^{32} \sin\left(\frac{k}{2} x_1\right).$$

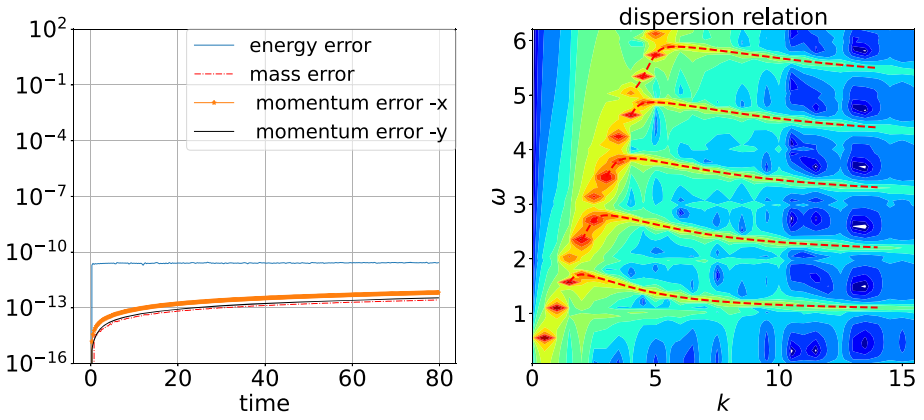

Fig. 3 Bernstein waves The formulation with isothermal electrons. Left figure: time evolution of the errors of mass. momentum, and energy. Right figure: the dispersion relation of the Bernstein waves.

The computational parameters are: grid number $64 \times 128 \times 128$, domain $[0, 4\pi] \times [-3, 3] \times [-3, 3]$, time step size $\Delta t = 0.05$, $v_T = 0.4$, final computation time 80. We used cubic splines interpolation for the velocity advections in sub-step pvb, and Fourier spectral method for the space advections in sub-stpe xv.

For the isothermal electron case with $\kappa = 0.09$, we use the Strang splitting $\phi_{xv}^{\frac{\Delta t}{2}} \phi_{pvb}^{\Delta t} \phi_{xv}^{\frac{\Delta t}{2}}$ [16]. We show the the time evolutions of energy error, momentum errors, and mass error, and the dispersion relations of Bernstein waves in Fig. 3. The errors of mass, momentum, and energy are around 10^{-13}, 10^{-13}, and 10^{-11}, respectively. The red lines in the second figure of Fig. 3 denote the analytical dispersion relation obtained by the Python package HYDROS [42], and we can see that our numerical results fit in well with the analytical dispersion relation.

Next, we consider the case with the electron pressure equation and $\gamma = 5/3$ with the Strang splitting $\phi_{xv}^{\frac{\Delta t}{2}} \phi_{pvb}^{\Delta t} \phi_{xv}^{\frac{\Delta t}{2}}$ [16]. We use the same initial condition as above and the initial value of the electron pressure is $p(x_1) = 0.09$. Note that with the initial condition we choose, the hybrid model with the electron pressure equation is equivalent to the hybrid model with adiabatic electrons, $\gamma = 5/3$, and $p = 0.09\rho^\gamma$. On the numerical side, we should also preserve the relation $p = 0.09\rho^\gamma$ as much as possible.

The computation parameters are the same as in the isothermal electron case. The results are presented in Fig. 4. We can see the energy is conserved with an error around 10^{-12}. Mass and momentum errors are around 10^{-13}. In the second figure, we can see several branches of the numerical dispersion relation, each branch becomes flat when the wave number becomes large, which is classical in the dispersion relation of Bernstein waves. These branches fit in well with the red lines, which denote the analytical dispersion relation of the hybrid model with adiabatic electrons by HYDROS [42]. The error in l_1 norm (around 10^{-8}) of the relation $p = 0.09\rho^\gamma$ is shown in the first figure in Fig. 4. It is also important to note that for general electrons, i.e., non-isothermal and non-adiabatic electrons, there is no such relation that must be conserved numerically.

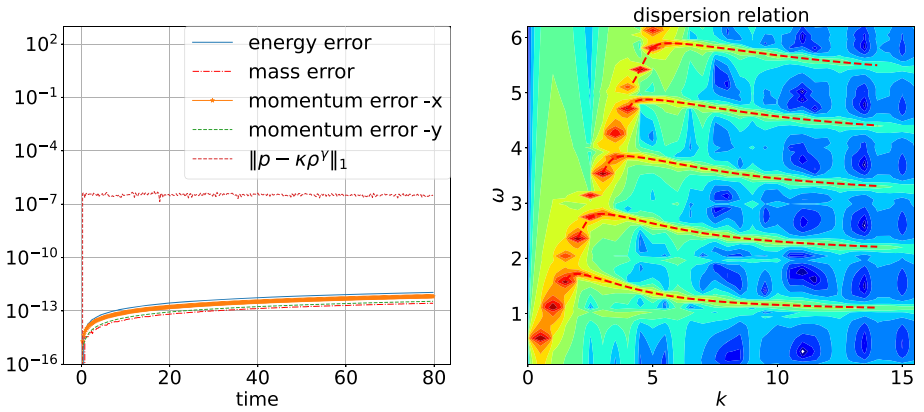

Fig. 4 **Bernstein waves** The formulation with the electron pressure equation. Left figure: Time evolution of $\|p - \kappa\rho^\gamma\|_1$ and the errors of mass, momentum, and energy. Right figure: the dispersion relation of the Bernstein waves.

7 Conclusion

In this work, the cubic spline based semi-Lagrangian methods [38] are used to solve the hybrid model with kinetic ions and massless electrons. Thanks to the exact splitting constructed, the Poisson splitting [21], based on the Poisson bracket [30, 43], yields only two sub-steps. For the complicated sub-step involving the update of the kinetic velocity with the mean fluid velocity, a specially designed mean velocity is chosen to ensure good conservation properties. The entire scheme is efficient, as it requires only one-dimensional advections for the distribution functions, with nonlinear iterations applied solely to the field unknowns. The scheme conserves mass, momentum, and energy, while also preserving the divergence-free condition of the magnetic field and overcome the cancellation problem [40]. These conservation properties are validated through numerical experiments on Landau damping and Bernstein waves.

We are implementing the algorithms proposed in this work within Gyselalib++ [6, 15], with the aim of subsequent physical applications. Other future work includes applying the exact splitting to other electro-magnetic models, developing efficient solvers for the nonlinear systems, performing simulations on domains with complex geometries, exploring other discretization methods, such as the numerical methods in the framework of finite element exterior calculus [2] and discrete exterior calculus [12].

Acknowledgements Simulations in this work were performed on Max Planck Computing & Data Facility (MPCDF). The authors would like to acknowledge Omar Maj for the kind discussions about Bernstein waves and Stefan Possanner for the fruitful discussions on this model over the years.

Funding Open Access funding enabled and organized by Projekt DEAL. Philip J. Morrison received support from the DOE Office of Fusion Energy Sciences under DE-FG02-04ER-54742.

Data Availibility The code and data used in this work are available upon request.

Declarations

Conflicts of Interest The authors declare that they have no conflict of interest.

8 Appendix

8.1 Poisson Brackets of the Hybrid Model

$$
\begin{aligned}
\{\mathcal{F},\mathcal{G}\}_{pvb} = &-\int f(\boldsymbol{v})\, f(\boldsymbol{v}')\, \frac{\boldsymbol{B}}{\rho}\cdot\left(\nabla_v \frac{\delta\mathcal{F}}{\delta f}\times\nabla_{v'}\frac{\delta\mathcal{G}}{\delta f}\right)\mathrm{d}\boldsymbol{x}\,\mathrm{d}\boldsymbol{v}\,\mathrm{d}\boldsymbol{v}' \\
&+\int f\boldsymbol{B}\cdot\nabla_v\frac{\delta\mathcal{F}}{\delta f}\times\nabla_v\frac{\delta\mathcal{G}}{\delta f}\,\mathrm{d}\boldsymbol{x}\,\mathrm{d}\boldsymbol{v}-\int\frac{\boldsymbol{B}}{\rho}\cdot\left(\nabla\times\frac{\delta\mathcal{F}}{\delta\boldsymbol{B}}\right)\times\left(\nabla\times\frac{\delta\mathcal{G}}{\delta\boldsymbol{B}}\right)\mathrm{d}\boldsymbol{x} \\
&+\int\frac{f}{\rho}\boldsymbol{B}\cdot\left[\nabla_v\frac{\delta\mathcal{F}}{\delta f}\times\left(\nabla\times\frac{\delta\mathcal{G}}{\delta\boldsymbol{B}}\right)-\nabla_v\frac{\delta\mathcal{G}}{\delta f}\times\left(\nabla\times\frac{\delta\mathcal{F}}{\delta\boldsymbol{B}}\right)\right]\mathrm{d}\boldsymbol{x}\,\mathrm{d}\boldsymbol{v} \\
&+\int\gamma p\left(\frac{\delta\mathcal{F}}{\delta p}\nabla\cdot\frac{\nabla\times\frac{\delta\mathcal{G}}{\delta\boldsymbol{B}}-\int f\,\nabla_v\frac{\delta\mathcal{G}}{\delta f}\,\mathrm{d}\boldsymbol{v}}{\rho}-\frac{\delta\mathcal{G}}{\delta p}\nabla\cdot\frac{\nabla\times\frac{\delta\mathcal{F}}{\delta\boldsymbol{B}}-\int f\,\nabla_v\frac{\delta\mathcal{F}}{\delta f}\,\mathrm{d}\boldsymbol{v}}{\rho}\right)\mathrm{d}\boldsymbol{x} \\
&+\int\frac{\nabla p}{\rho}\cdot\left(\frac{\delta\mathcal{F}}{\delta p}\left(\nabla\times\frac{\delta\mathcal{G}}{\delta\boldsymbol{B}}-\int f\,\nabla_v\frac{\delta\mathcal{G}}{\delta f}\mathrm{d}\boldsymbol{v}\right)-\frac{\delta\mathcal{G}}{\delta p}\left(\nabla\times\frac{\delta\mathcal{F}}{\delta\boldsymbol{B}}-\int f\,\nabla_v\frac{\delta\mathcal{F}}{\delta f}\mathrm{d}\boldsymbol{v}\right)\right)\mathrm{d}\boldsymbol{x}, \\
\{\mathcal{F},\mathcal{G}\}_{xv} = &\int f\left(\nabla_x\frac{\delta\mathcal{F}}{\delta f}\cdot\nabla_v\frac{\delta\mathcal{G}}{\delta f}-\nabla_v\frac{\delta\mathcal{F}}{\delta f}\cdot\nabla_x\frac{\delta\mathcal{G}}{\delta f}\right)\mathrm{d}\boldsymbol{x}\,\mathrm{d}\boldsymbol{v}.
\end{aligned}
$$

8.2 Partial Discrete Fourier Transformations

For a scalar function $\mathbf{s}$ defined on grid $\mathbb{G}^x$, we define partial discrete Fourier transformations as [4]

$$
\mathcal{F}_1 : \begin{cases} \mathbb{C}^{\mathbb{G}^x} \to \mathbb{C}^{\hat{\mathbb{G}}^{x_1}\times\mathbb{G}^{x_2}\times\mathbb{G}^{x_3}} \\ \mathbf{s} \to \sum\limits_{\mathsf{x}_1\in\mathbb{G}^{x_1}} \mathbf{s}_{\mathsf{x}_1,\mathsf{x}_2,\mathsf{x}_3} e^{-\mathrm{i}\mathsf{x}_1\xi_1}, \end{cases}
$$

$$
\mathcal{F}_2 : \begin{cases} \mathbb{C}^{\mathbb{G}^x} \to \mathbb{C}^{\mathbb{G}^{x_1}\times\hat{\mathbb{G}}^{x_2}\times\mathbb{G}^{x_3}} \\ \mathbf{s} \to \sum\limits_{\mathsf{x}_2\in\mathbb{G}^{x_2}} \mathbf{s}_{\mathsf{x}_1,\mathsf{x}_2,\mathsf{x}_3} e^{-\mathrm{i}\mathsf{x}_2\xi_2}, \end{cases}
$$

$$
\mathcal{F}_3 : \begin{cases} \mathbb{C}^{\mathbb{G}^x} \to \mathbb{C}^{\mathbb{G}^{x_1}\times\mathbb{G}^{x_2}\times\hat{\mathbb{G}}^{x_3}} \\ \mathbf{s} \to \sum\limits_{\mathsf{x}_3\in\mathbb{G}^{x_3}} \mathbf{s}_{\mathsf{x}_1,\mathsf{x}_2,\mathsf{x}_3} e^{-\mathrm{i}\mathsf{x}_3\xi_3}. \end{cases}
$$

8.3 Discrete Operators of ∇, $\nabla\times$, $\nabla\cdot$

$$\nabla : \begin{cases} \mathbb{C}^{\mathbb{G}^x} \to \mathbb{C}^{\mathbb{G}^x} \times \mathbb{C}^{\mathbb{G}^x} \times \mathbb{C}^{\mathbb{G}^x} \\ \mathbf{s} \to (\mathcal{F}_1^{-1}[\mathrm{i}\xi_1\mathcal{F}_1\mathbf{s}], \mathcal{F}_2^{-1}[\mathrm{i}\xi_2\mathcal{F}_2\mathbf{s}], \mathcal{F}_3^{-1}[\mathrm{i}\xi_3\mathcal{F}_3\mathbf{s}])^\top \end{cases},$$

$$\nabla\times : \begin{cases} \mathbb{C}^{\mathbb{G}^x} \times \mathbb{C}^{\mathbb{G}^x} \times \mathbb{C}^{\mathbb{G}^x} \to \mathbb{C}^{\mathbb{G}^x} \times \mathbb{C}^{\mathbb{G}^x} \times \mathbb{C}^{\mathbb{G}^x} \\ \mathbf{B} \to \begin{pmatrix} \mathcal{F}_2^{-1}[\mathrm{i}\xi_2\mathcal{F}_2\mathbf{B}_3] - \mathcal{F}_3^{-1}[\mathrm{i}\xi_3\mathcal{F}_3\mathbf{B}_2] \\ \mathcal{F}_3^{-1}[\mathrm{i}\xi_3\mathcal{F}_3\mathbf{B}_1] - \mathcal{F}_1^{-1}[\mathrm{i}\xi_1\mathcal{F}_1\mathbf{B}_3] \\ \mathcal{F}_1^{-1}[\mathrm{i}\xi_1\mathcal{F}_1\mathbf{B}_2] - \mathcal{F}_2^{-1}[\mathrm{i}\xi_2\mathcal{F}_2\mathbf{B}_1] \end{pmatrix} \end{cases},$$

$$\nabla\cdot : \begin{cases} \mathbb{C}^{\mathbb{G}^x} \times \mathbb{C}^{\mathbb{G}^x} \times \mathbb{C}^{\mathbb{G}^x} \to \mathbb{C}^{\mathbb{G}^x} \\ \mathbf{B} \to \mathcal{F}_1^{-1}[\mathrm{i}\xi_1\mathcal{F}_1\mathbf{B}_1] + \mathcal{F}_2^{-1}[\mathrm{i}\xi_2\mathcal{F}_2\mathbf{B}_2] + \mathcal{F}_3^{-1}[\mathrm{i}\xi_3\mathcal{F}_3\mathbf{B}_3] \end{cases}.$$

We calculate $\nabla \times \nabla\mathbf{s}$ directly, the first component of which is

$$\begin{aligned} &\mathcal{F}_2^{-1}[\mathrm{i}\xi_2\mathcal{F}_2\left(\mathcal{F}_3^{-1}[\mathrm{i}\xi_3\mathcal{F}_3\mathbf{s}]\right)] - \mathcal{F}_3^{-1}[\mathrm{i}\xi_3\mathcal{F}_3\left(\mathcal{F}_2^{-1}[\mathrm{i}\xi_2\mathcal{F}_2\mathbf{s}]\right)] \\ &= \mathcal{F}_3^{-1}\mathcal{F}_2^{-1}[\mathrm{i}\xi_2\mathrm{i}\xi_3\mathcal{F}_3\mathcal{F}_2\mathbf{s}] - \mathcal{F}_3^{-1}\mathcal{F}_2^{-1}[\mathrm{i}\xi_2\mathrm{i}\xi_3\mathcal{F}_3\mathcal{F}_2\mathbf{s}] = 0. \end{aligned}$$

The second component of $\nabla \times \nabla\mathbf{s}$ is

$$\begin{aligned} &\mathcal{F}_3^{-1}[\mathrm{i}\xi_3\mathcal{F}_3\left(\mathcal{F}_1^{-1}[\mathrm{i}\xi_1\mathcal{F}_1\mathbf{s}]\right)] - \mathcal{F}_1^{-1}[\mathrm{i}\xi_1\mathcal{F}_1\left(\mathcal{F}_3^{-1}[\mathrm{i}\xi_3\mathcal{F}_3\mathbf{s}]\right)] \\ &= \mathcal{F}_3^{-1}\mathcal{F}_1^{-1}[\mathrm{i}\xi_3\mathrm{i}\xi_1\mathcal{F}_3\mathcal{F}_1\mathbf{s}] - \mathcal{F}_3^{-1}\mathcal{F}_1^{-1}[\mathrm{i}\xi_3\mathrm{i}\xi_1\mathcal{F}_3\mathcal{F}_1\mathbf{s}] = 0. \end{aligned}$$

The third component of $\nabla \times \nabla\mathbf{s}$ is

$$\begin{aligned} &\mathcal{F}_1^{-1}[\mathrm{i}\xi_1\mathcal{F}_1\left(\mathcal{F}_2^{-1}[\mathrm{i}\xi_2\mathcal{F}_2\mathbf{s}]\right)] - \mathcal{F}_2^{-1}[\mathrm{i}\xi_2\mathcal{F}_2\left(\mathcal{F}_1^{-1}[\mathrm{i}\xi_1\mathcal{F}_1\mathbf{s}]\right)] \\ &= \mathcal{F}_2^{-1}\mathcal{F}_1^{-1}[\mathrm{i}\xi_2\mathrm{i}\xi_1\mathcal{F}_2\mathcal{F}_1\mathbf{s}] - \mathcal{F}_2^{-1}\mathcal{F}_1^{-1}[\mathrm{i}\xi_2\mathrm{i}\xi_1\mathcal{F}_2\mathcal{F}_1\mathbf{s}] = 0. \end{aligned}$$

Then we have proved that $\nabla \times \nabla = 0$.

Next, we calculate $\nabla \cdot \nabla \times \mathbf{B}$ directly and obtain

$$\begin{aligned} \nabla \cdot \nabla \times \mathbf{B} &= \mathcal{F}_1^{-1}[\mathrm{i}\xi_1\mathcal{F}_1(\nabla \times \mathbf{B})_1] + \mathcal{F}_2^{-1}[\mathrm{i}\xi_2\mathcal{F}_2(\nabla \times \mathbf{B})_2] + \mathcal{F}_3^{-1}[\mathrm{i}\xi_3\mathcal{F}_3(\nabla \times \mathbf{B})_3] \\ &= \mathcal{F}_1^{-1}[\mathrm{i}\xi_1\mathcal{F}_1\left(\mathcal{F}_2^{-1}[\mathrm{i}\xi_2\mathcal{F}_2\mathbf{B}_3] - \mathcal{F}_3^{-1}[\mathrm{i}\xi_3\mathcal{F}_3\mathbf{B}_2]\right)] \\ &\quad + \mathcal{F}_2^{-1}[\mathrm{i}\xi_2\mathcal{F}_2\left(\mathcal{F}_3^{-1}[\mathrm{i}\xi_3\mathcal{F}_3\mathbf{B}_1] - \mathcal{F}_1^{-1}[\mathrm{i}\xi_1\mathcal{F}_1\mathbf{B}_3]\right)] \\ &\quad + \mathcal{F}_3^{-1}[\mathrm{i}\xi_3\mathcal{F}_3\left(\mathcal{F}_1^{-1}[\mathrm{i}\xi_1\mathcal{F}_1\mathbf{B}_2] - \mathcal{F}_2^{-1}[\mathrm{i}\xi_2\mathcal{F}_2\mathbf{B}_1]\right)] \\ &= \mathcal{F}_1^{-1}\mathcal{F}_2^{-1}[\mathrm{i}\xi_1\mathrm{i}\xi_2\mathcal{F}_1\mathcal{F}_2\mathbf{B}_3] - \mathcal{F}_1^{-1}\mathcal{F}_3^{-1}[\mathrm{i}\xi_1\mathrm{i}\xi_3\mathcal{F}_1\mathcal{F}_3\mathbf{B}_2] \\ &\quad + \mathcal{F}_2^{-1}\mathcal{F}_3^{-1}[\mathrm{i}\xi_2\mathrm{i}\xi_3\mathcal{F}_2\mathcal{F}_3\mathbf{B}_1] - \mathcal{F}_1^{-1}\mathcal{F}_2^{-1}[\mathrm{i}\xi_1\mathrm{i}\xi_2\mathcal{F}_1\mathcal{F}_2\mathbf{B}_3] \\ &\quad + \mathcal{F}_1^{-1}\mathcal{F}_3^{-1}[\mathrm{i}\xi_1\mathrm{i}\xi_3\mathcal{F}_1\mathcal{F}_3\mathbf{B}_2] - \mathcal{F}_2^{-1}\mathcal{F}_3^{-1}[\mathrm{i}\xi_2\mathrm{i}\xi_3\mathcal{F}_2\mathcal{F}_3\mathbf{B}_1] \\ &= 0, \end{aligned}$$

by which we have proved that $\nabla \cdot \nabla\times = 0$.

References

1. Acheson, D.J.: Elementary fluid dynamics, Oxford University Press (1990)
2. Arnold, D.N., Falk, R.S., Winther, R.: Finite element exterior calculus, homological techniques, and applications. Acta Numer **15**, 1–155 (2006)
3. Bernier, J.: Exact splitting methods for semigroups generated by inhomogeneous quadratic differential operators. Found. Comput. Math. **21**(5), 1401–1439 (2021)
4. Bernier, J., Casas, F., Crouseilles, N.: Splitting methods for rotations: application to Vlasov equations. SIAM J. Sci. Comput. **42**(2), A666–A697 (2020)
5. Bernier, J., Crouseilles, N., Li, Y.: Exact splitting methods for kinetic and Schrödinger equations. J. Sci. Comput. **86**, 1–35 (2021)
6. Bourne, E., Grandgirard, V., Asahi, Y., Bigot, J., Donnel, P., Hoffmann, A., Kara, A., Krah, P., Legouix, B., Malaboeuf, E., et al.: Gyselalib++: a portable C++ library for semi-Lagrangian kinetic and gyrokinetic simulations. Journal of Open Source Software **10**(113), 8582 (2025)
7. Campos Pinto, M., Kormann, K., Sonnendrücker, E.: Variational framework for structure-preserving electromagnetic particle-in-cell methods. J. Sci. Comput. **91**(2), 46 (2022)
8. Chen, B., Kaufman, A.: 3d volume rotation using shear transformations. Graph. Models **62**(4), 308–322 (2000)
9. Cheng, C.Z., Knorr, G.: The integration of the Vlasov equation in configuration space. J. Comput. Phys. **22**(3), 330–351 (1976)
10. Crouseilles, N., Einkemmer, L., Faou, E.: Hamiltonian splitting for the Vlasov-Maxwell equations. J. Comput. Phys. **283**, 224–240 (2015)
11. Crouseilles, N., Mehrenberger, M., Sonnendrücker, E.: Conservative semi-Lagrangian schemes for Vlasov equations. J. Comput. Phys. **229**(6), 1927–1953 (2010)
12. Desbrun, M., Hirani, A.N., Leok, M., Marsden, J.E.: Discrete exterior calculus, (2005). math/0508341 arXiv preprint
13. Filbet, F., Sonnendrücker, E., Bertrand, P.: Conservative numerical schemes for the Vlasov equation. J. Comput. Phys. **172**(1), 166–187 (2001)
14. Franci, L., Hellinger, P., Guarrasi, M., Chen, C., Papini, E., Verdini, A., Matteini, L., Landi, S.: Three-dimensional simulations of solar wind turbulence with the hybrid code CAMELIA. J. Phys: Conf. Ser. **1031**, 012002 (2018). (**IOP Publishing**)
15. Grandgirard, V., Abiteboul, J., Bigot, J., Cartier-Michaud, T., Crouseilles, N., Dif-Pradalier, G., Ehrlacher, C., Esteve, D., Garbet, X., Ghendrih, P., et al.: A 5d gyrokinetic full-f global semi-lagrangian code for flux-driven ion turbulence simulations. Comput. Phys. Commun. **207**, 35–68 (2016)
16. Hairer, E., Hochbruck, M., Iserles, A., Lubich, C.: Geometric numerical integration. Oberwolfach Reports **3**(1), 805–882 (2006)
17. He, Y., Qin, H., Sun, Y., Xiao, J., Zhang, R., Liu, J.: Hamiltonian time integrators for Vlasov-Maxwell equations. Phys. Plasmas **22**(12), (2015)
18. He, Y., Sun, Y., Liu, J., Qin, H.: Volume-preserving algorithms for charged particle dynamics. J. Comput. Phys. **281**, 135–147 (2015)
19. He, Y., Sun, Y., Qin, H., Liu, J.: Hamiltonian particle-in-cell methods for Vlasov-Maxwell equations. Phys. Plasmas **23**(9), (2016)
20. Huot, F., Ghizzo, A., Bertrand, P., Sonnendrücker, E., Coulaud, O.: Instability of the time splitting scheme for the one-dimensional and relativistic Vlasov-Maxwell system. J. Comput. Phys. **185**(2), 512–531 (2003)
21. Kormann, K., Sonnendrücker, E.: Energy-conserving time propagation for a structure-preserving particle-in-cell Vlasov-Maxwell solver. J. Comput. Phys. **425**, 109890 (2021)
22. Kormann, K., Sonnendrücker, E.: A Dual Grid Geometric Electromagnetic Particle in Cell Method. SIAM J. Sci. Comput. **46**(5), B621–B646 (2024)
23. Kraus, M., Kormann, K., Morrison, P.J., Sonnendrücker, E.: GEMPIC: geometric electromagnetic particle-in-cell methods. J. Plasma Phys. **83**(4), 905830401 (2017)
24. Kunz, M.W., Stone, J.M., Bai, X.N.: Pegasus: a new hybrid-kinetic particle-in-cell code for astrophysical plasma dynamics. J. Comput. Phys. **259**, 154–174 (2014)
25. Lapenta, G.: Exactly energy conserving semi-implicit particle in cell formulation. J. Comput. Phys. **334**, 349–366 (2017)
26. Le, A., Stanier, A., Yin, L., Wetherton, B., Keenan, B., Albright, B.: Hybrid-VPIC: An open-source kinetic/fluid hybrid particle-in-cell code. Phys. Plasmas 30(6), (2023)
27. Li, Y., Campos Pinto, M., Holderied, F., Possanner, S., Sonnendrücker, E.: Geometric particle-in-cell discretizations of a plasma hybrid model with kinetic ions and mass-less fluid electrons. J. Comput. Phys. **498**, 112671 (2024)

28. Li, Y., He, Y., Sun, Y., Niesen, J., Qin, H., Liu, J.: Solving the Vlasov-Maxwell equations using Hamiltonian splitting. J. Comput. Phys. **396**, 381–399 (2019)
29. Li, Y., Holderied, F., Possanner, S., Sonnendrücker, E.: Canonical variables based numerical schemes for hybrid plasma models with kinetic ions and massless electrons. J. Comput. Phys. **505**, 112916 (2024)
30. Li, Y., Morrison, P. J., Possanner, S., & Sonnendrücker, E.: On the Poisson brackets of hybrid plasma models with kinetic ions and massless electrons. Phys. Plasmas. **33**(7), 072103 (2026). https://doi.org/10.1063/5.0332100
31. Liu, H., Cai, X., Cao, Y., Lapenta, G.: An efficient energy conserving semi-lagrangian kinetic scheme for the Vlasov-Ampère system. J. Comput. Phys. **492**, 112412 (2023)
32. Matthews, A.P.: Current advance method and cyclic leapfrog for 2D multispecies hybrid plasma simulations. J. Comput. Phys. **112**(1), 102–116 (1994)
33. McLachlan, R.I., Quispel, G.R.W.: Splitting methods. Acta Numer **11**, 341–434 (2002)
34. Palmroth, M., Ganse, U., Pfau-Kempf, Y., Battarbee, M., Turc, L., Brito, T., Grandin, M., Hoilijoki, S., Sandroos, A., von Alfthan, S.: Vlasov methods in space physics and astrophysics. Living reviews in computational astrophysics **4**(1), 1 (2018)
35. Qin, H., He, Y., Zhang, R., Liu, J., Xiao, J., Wang, Y.: Comment on "Hamiltonian splitting for the Vlasov-Maxwell equations". J. Comput. Phys. **297**, 721–723 (2015)
36. Shen, J., Tang, T., Wang, L.L.: Spectral methods: algorithms, analysis and applications, vol. 41. Springer Science & Business Media (2011)
37. Sonnendrücker, E.: Numerical methods for the Vlasov-Maxwell equations. (**to appear**)
38. Sonnendrücker, E., Roche, J., Bertrand, P., Ghizzo, A.: The semi-lagrangian method for the numerical resolution of the Vlasov equation. J. Comput. Phys. **149**(2), 201–220 (1999)
39. Stanier, A., Chacón, L., Chen, G.: A fully implicit, conservative, non-linear, electromagnetic hybrid particle-ion/fluid-electron algorithm. J. Comput. Phys. **376**, 597–616 (2019)
40. Stanier, A., Chacon, L., Le, A.: A cancellation problem in hybrid particle-in-cell schemes due to finite particle size. J. Comput. Phys. **420**, 109705 (2020)
41. Strang, G.: On the construction and comparison of difference schemes. SIAM J. Numer. Anal. **5**(3), 506–517 (1968)
42. Told, D., Cookmeyer, J., Astfalk, P., Jenko, F.: A linear dispersion relation for the hybrid kinetic-ion/fluid-electron model of plasma physics. New J. Phys. **18**(7), 075001 (2016)
43. Tronci, C.: Hamiltonian approach to hybrid plasma models. J. Phys. A: Math. Theor. **43**(37), 375501 (2010)
44. Udovicic, Z.: Calculation of the moments of the cardinal b-spline. Sarajevo journal of mathematics **5**(18), 291–297 (2009)
45. Valentini, F., Trávníček, P., Califano, F., Hellinger, P., Mangeney, A.: A hybrid-Vlasov model based on the current advance method for the simulation of collisionless magnetized plasma. J. Comput. Phys. **225**(1), 753–770 (2007)
46. Von Alfthan, S., Pokhotelov, D., Kempf, Y., Hoilijoki, S., Honkonen, I., Sandroos, A., Palmroth, M.: Vlasiator: First global hybrid-Vlasov simulations of Earth's foreshock and magnetosheath. J. Atmos. Solar Terr. Phys. **120**, 24–35 (2014)
47. Welling, J.S., Eddy, W.F., Young, T.K.: Rotation of 3d volumes by Fourier-interpolated shears. Graph. Models **68**(4), 356–370 (2006)
48. Winske, D., Yin, L., Omidi, N., Karimabadi, H., Quest, K.: Hybrid simulation codes: Past, present and future-A tutorial. Space plasma simulation pp. 136–165 (2003)
49. Xiao, J., Qin, H., Liu, J., He, Y., Zhang, R., Sun, Y.: Explicit high-order non-canonical symplectic particle-in-cell algorithms for Vlasov-Maxwell systems. Phys. Plasmas **22**(11), (2015)
50. Xiong, T., Qiu, J.M., Xu, Z., Christlieb, A.: High order maximum principle preserving semi-Lagrangian finite difference WENO schemes for the Vlasov equation. J. Comput. Phys. **273**, 618–639 (2014)